AERODYNAMICS OF ROAD VEHICLES

Wolf-Heinrich Hucho

Ostring 48, D-6231, Schwalbach (Ts), Germany

Gino Sovran

General Motors Research and Environmental Staff, Warren, Michigan 48090-9055

1. INTRODUCTION

In fluid mechanical terms, road vehicles are bluff bodies in very close proximity to the ground. Their detailed geometry is extremely complex. Internal and recessed cavities which communicate freely with the external flow (i.e. engine compartment and wheel wells, respectively) and rotating wheels add to their geometrical and fluid mechanical complexity. The flow over a vehicle is fully three-dimensional. Boundary layers are turbulent. Flow separation is common and may be followed by reattachment. Large turbulent wakes are formed at the rear and in many cases contain longitudinal trailing vortices.

As is typical for bluff bodies, drag (which is a key issue for most road vehicles—but far from the only one) is mainly pressure drag. This is in contrast to aircraft and ships, which suffer primarily from friction drag. The avoidance of separation or, if this is not possible, its control are among the main objectives of vehicle aerodynamics.

With regard to their geometry, road vehicles comprise a large variety of configurations (Figure 1). Passenger cars, vans, and buses are closed, single bodies. Trucks and race cars can be of more than one body. Motorcycles and some race cars have open driver compartments. With the race car being the only exception, the shape of a road vehicle is not primarily

485
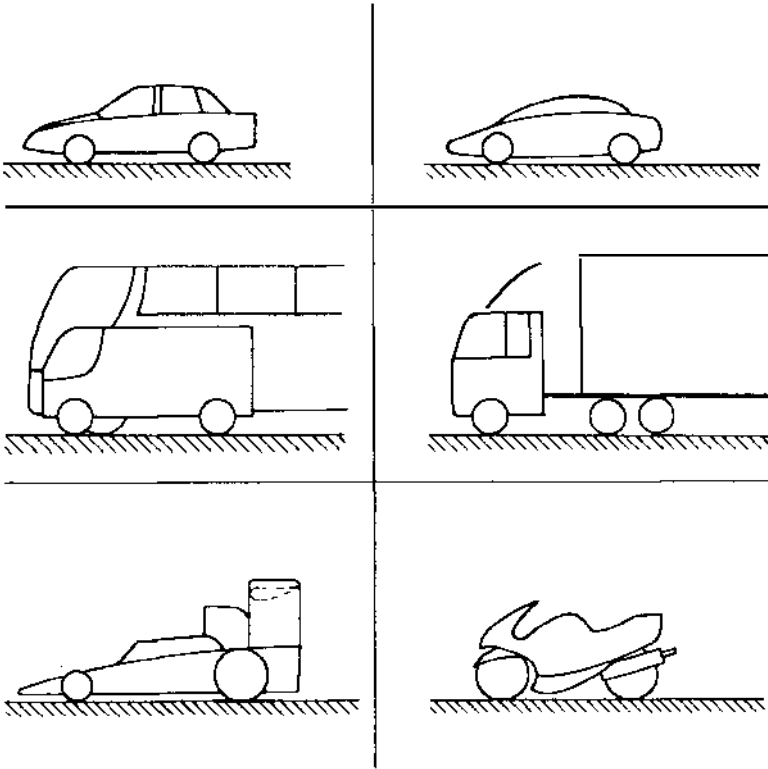
Figure 1 With respect to geometry, road vehicles comprise a wide variety of shapes. Race cars and, even more so, motorcycles have to be studied with the driver in place.

determined by the need to generate specific aerodynamic effects—as, for instance, an airplane is designed to produce lift.

To the contrary, a road vehicle's shape is primarily determined by functional, economic and, last but not least, aesthetic arguments. The aerodynamic characteristics are not usually generated intentionally; they are the consequences of, but not the reason for, the shape. These "other than aerodynamic" considerations place severe constraints on vehicle aerodynamicists. For example, there are good reasons for the length of a vehicle being a given. Length for a passenger car is a measure of its size, and thus its class. To place a car in a specific market niche means recognizing length as an invariant in design. Furthermore, mass and cost are proportional to length. In the same sense all the other main dimensions of a vehicle, such as width and height (which define frontal area), are frozen very early in the design process. Even the details of a car's proportions are prescribed

to close limits for reasons of packaging and aesthetics (Figure 2). Of course, some maneuvering room must be left to the aerodynamicists (the hatched regions). Otherwise, they would do no more than just measure the aerodynamic characteristics of configurations designed by others.

Depending on the specific purpose of each type of vehicle, the objectives of aerodynamics differ widely. While low drag is desirable for all road vehicles, other aerodynamic properties are also significant. Negative lift is decisive for the cornering capability of race cars, but is of no importance for trucks. Cars and, even more so, vans are sensitive to cross wind, but heavy trucks are not. Wind noise should be low for cars and buses, but is of no significance for race cars.

While the process of weighing the relative importance of a set of needs from various disciplines is generally comparable to that in other branches of applied fluid mechanics, the situation in vehicle aerodynamics is unique in that an additional category of arguments has to be taken into account: art, fashion, and taste. In contrast to technical and economic factors, these additional arguments are subjective in nature and cannot be quantified.

Exterior design (the term "styling" that was formerly used is today usually avoided) has to be recognized as extremely important. "Design is what sells" rules the car market worldwide. While design gives technical requirements a form that is in accord with fashion, the fundamental nature
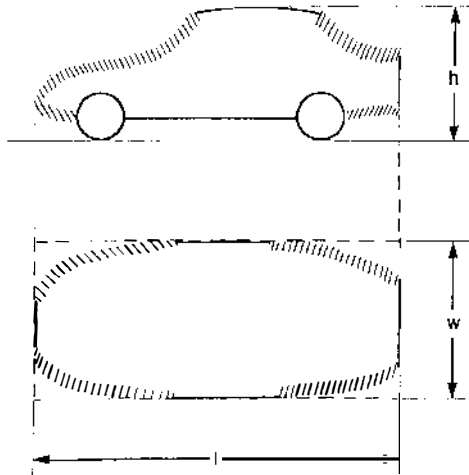
Figure 2   Right from the beginning of the development of a new vehicle, its main dimensions and detailed proportions are frozen. The limited maneuvering room for aerodynamics is identified by the hatched lines.

of fashion is change. Consequently, although vehicle aerodynamics is getting better and better, it is not progressing toward a single ultimate shape as in the case, for instance, of subsonic transport aircraft. To the contrary, it must come to terms with new shapes again and again.

There is no question, however, that aerodynamics does influence design. The high trunk typical of notchback cars with low drag is the most striking example. Despite the fact that it tends to look "bulky," it had to be accepted by designers because of its favorable effect on drag—and the extra luggage space it provides. Today's cars are streamlined more than ever, and an "aero-look" has become a styling feature of its own.

2. HISTORY

When the carriage horse was replaced by a thermal engine more than 100 years ago, nobody thought about aerodynamics. The objective of the body shell of the now horseless carriage was, as before, to shelter the driver and passengers from wind, rain, and mud. The idea of applying aerodynamics to road vehicles came up much later, after flight technology had made considerable progress. For both airships and aircraft, streamlined shapes were developed which lowered drag significantly, thus permitting higher cruising speeds with any given (limited) engine power.

The early attempts (Figure 3) to streamline cars were made according to aeronautical practice and by adapting shapes from naval architecture. These failed for two reasons. First, the benefits of aerodynamics were simply not needed. Bad roads and low engine power only permitted moderate driving speeds. Second, the approach of directly transplanting (with almost no change) shapes which had been developed for aeronautical and marine purposes was not appropriate. These streamlined shapes could be accommodated only if some important details of car design were subordinated, e.g. engine location, or the layout of the passenger compartment.

The long road from those days to today's acceptance of aerodynamics in the automobile industry has been described in great detail (Kieselbach 1982a,b, 1983; Hucho 1987b). From this history, only those events which were decisive will be highlighted here. Acknowledging the danger of being superficial, only five will be identified.

1. The recognition that the pattern of flow around half a body of revolution is changed significantly when that half body is brought close to the ground (Klemperer 1922, Figure 4).
2. The truncation of a body's rear end (Koenig-Fachsenfeld et al 1936, Kamm et al 1934, Figure 4).
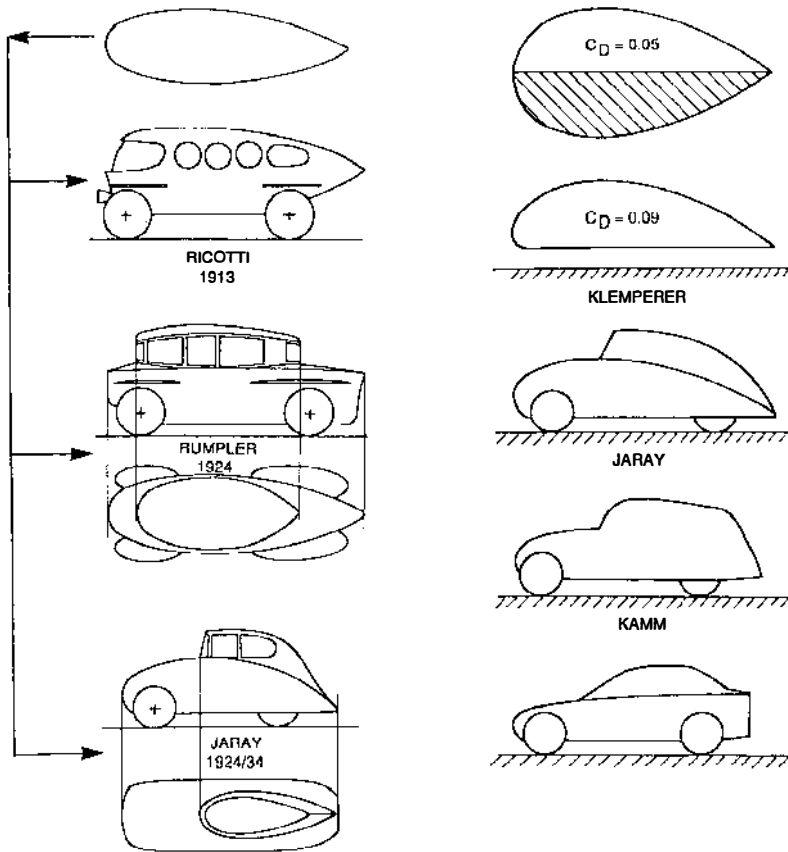
Figure 3 (*left*) The early attempts to apply aerodynamics to road vehicles consisted of the direct transfer of shapes originating from aeronautical and marine practice. The resulting shapes differed widely from those of contemporary cars and were rejected by the buying public. This unsuitable transfer procedure was very embarrassing for later attempts to introduce aerodynamics into vehicles.

Figure 4 (*right*) Klemperer (1922) recognized that the flow over a body of revolution, which is axisymmetric in free flight, changed drastically and lost symmetry when the body came close to the ground. By modifying its shape, however, he was able to reduce the related drag increase. Despite their extreme length, flow separates from the rear of streamlined cars. By truncating the rear shortly upstream of the location where separation would take place, shapes of acceptable length were generated with no drag penalty. This idea was first proposed by Koenig-Fachsenfeld for buses, and was transferred to cars by Kamm.

3 The introduction of "detail-optimization" into vehicle development (Figure 5, Hucho et al 1976).

4. The deciphering of the detailed flow patterns at car rear ends (Section 4.1).

5. The application of "add-ons" like underbody air dams, fairings, and wings to passenger cars, trucks, and race cars.

With these five steps, aerodynamics has been adapted to road vehicles, rather than road-vehicle configurations being determined by the demands of aerodynamics. The shape of cars changed in an evolutionary rather than a revolutionary manner over the years (Figure 6), and at first for reasons other than aerodynamic ones. Taste, perhaps influenced by the fascinating shapes of aircraft, called for smooth bodies with integrated headlamps and fenders (the "pontoon body"), and production technology made them possible. Better flow over the car and thus lower drag was only a spinoff. But, finally, the two oil crises of the 1970s generated great pressure for improving fuel economy drastically, and provided a break-
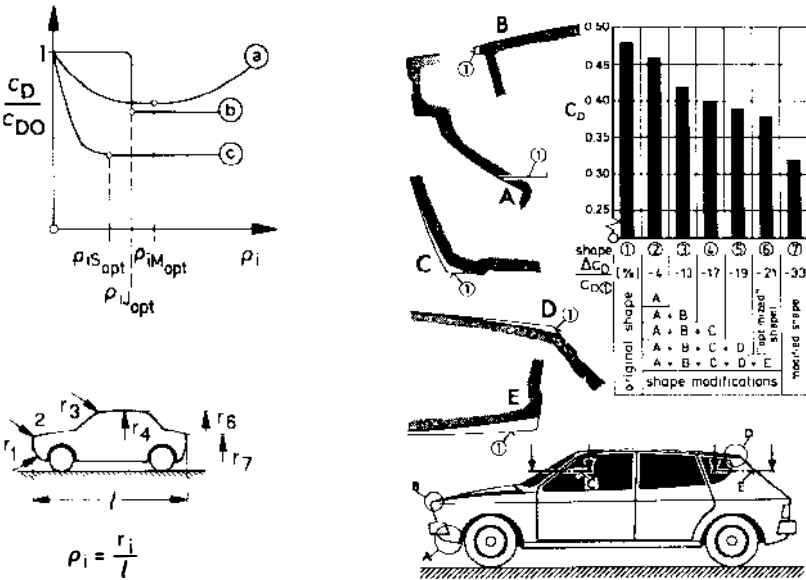

Figure 5 In detail optimization, a body detail is rounded off or tapered by no more than what is necessary to produce a drag minimum. In general, there are different types of drag variation that lead to such an optimum: (*a*) minimum; (*b*) jump; (*c*) saturation. Following this philosophy, it has been possible to significantly reduce the drag of hard-edged cars without altering their style.
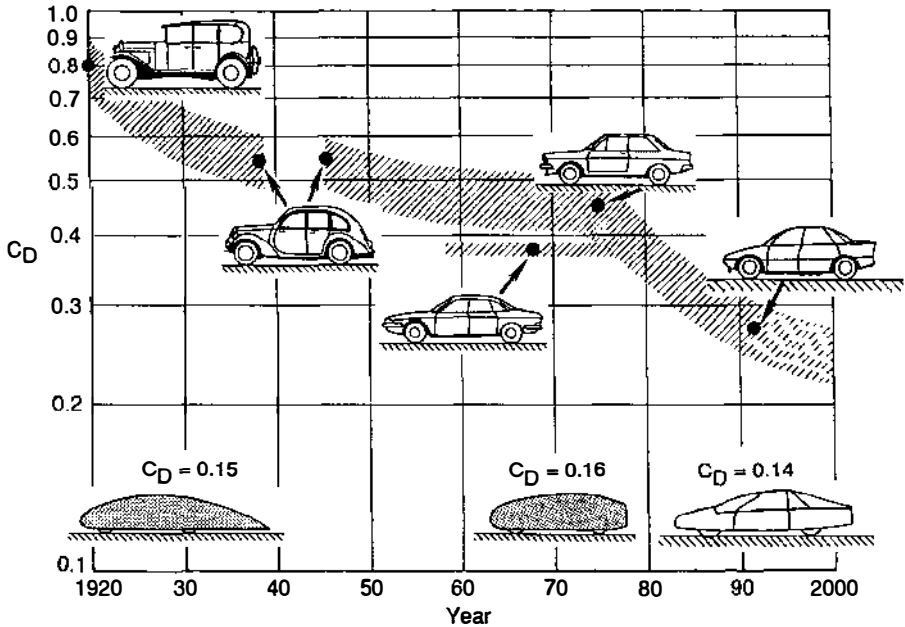
Figure 6 The drag history of cars. Using a logarithmic scale for drag emphasizes how difficult it is to achieve very low drag values. Research has been far ahead of what has been realized in production.

through for vehicle aerodynamics. Since then, drag coefficients have come down dramatically. This has been a major contributor to the large improvements in fuel economy that have been realized.

Research in road-vehicle aerodynamics has always been far ahead of practical application. Drag values demonstrate this. A drag coefficient as low as $C_D = 0.15$ was demonstrated for a body with wheels as early as 1922 (Klemperer, Figure 6), but it took more than 40 years to reproduce this value with an actual car—and then only with a research vehicle. Nevertheless, blaming the automobile industry for not taking advantage of the full potential of this technology is not justified, since the "concept" of any car is influenced by a variety of factors (Figure 7) which, collectively, are summarized by the term "market." However, the long-known potential for reducing drag (which relates to one of these factors) is now being exploited more and more. How far this trend will go depends on the future course of fuel prices and, perhaps, of emissions regulation (e.g. the possible regulation of CO_2 to control global warming).

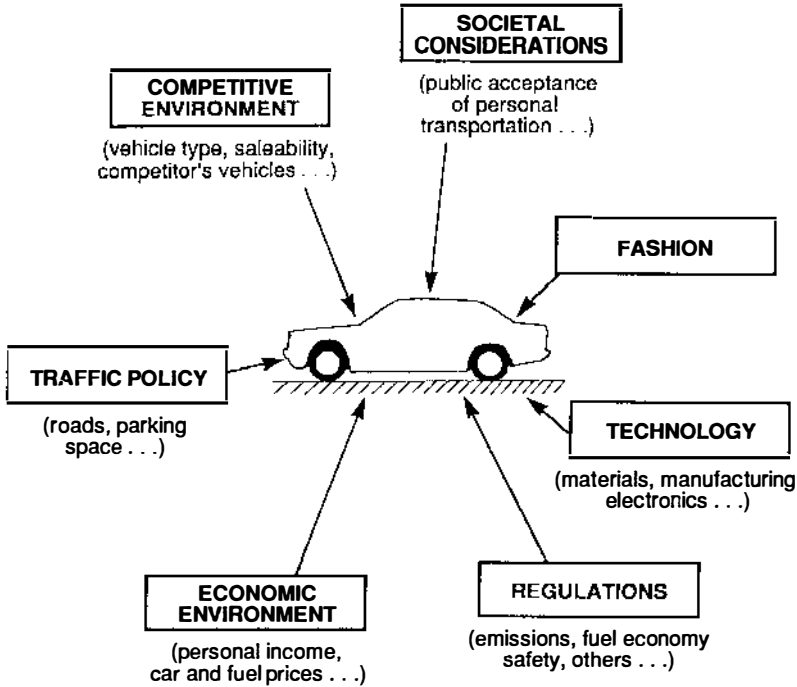In the following, the subject of road-vehicle aerodynamics will be treated

Figure 7   The concept of a car is influenced by many requirements of very different nature. A careful balance between them is required by the market.

in four sections. In the first (Section 3), the way that aerodynamics influences the operation of vehicles will be described, and without delving into the related fluid-mechanic mechanisms. These mechanisms will be discussed in a second section (Section 4). Then (Section 5), the aerodynamic-development process and the tools that are used in it will be described. In the final section (Section 6), open issues that remain and future trends will be discussed.

3.   VEHICLE ATTRIBUTES AFFECTED BY AERODYNAMICS

3.1   *Performance and Fuel Economy*

The motivation for allowing aerodynamics to influence the shape of vehicles, if not their style, is the market situation, and this changes with time. Fuel economy and, increasingly, global warming are the current key arguments for low drag worldwide. In Europe, particularly Germany, top

speed is still considered an important sales feature despite the rapidly increasing traffic density which largely prohibits fast driving even in the absence of speed limits.

Vehicle fuel consumption is a matter of demand and supply. On the demand side are the mechanical energies required for propulsion and by accessories. On the supply side is the efficiency with which this energy can be generated by the powerplant and delivered to the points of application. The influence of aerodynamics on this demand-supply relationship is through the drag force, which affects the propulsive part of the demand side.

Commercial aircraft, trains, ships, and highway trucks typically operate at a relatively constant cruising speed. In typical automobile driving, however, vehicle speed varies with time or distance. An analysis of the factors affecting automobile fuel economy can best be made if the driving pattern is prescribed. In the U.S., two speed variations of particular relevance are the Environmental Protection Agency (EPA) Urban and Highway schedules that are the basis for the fuel-economy and exhaust-emissions regulations. They represent the two major types of driving, and a combination of their fuel consumptions is used for regulatory purposes. In Europe, regulation is based on the Euromix cycle, a combination of a simple urban schedule and two constant-speed cruising conditions.

At any instant, the tractive force required at the tire/road interface of a car's driving wheels is (Sovran & Bohn 1981)

$$F_{TR} = \underbrace{R + D}_{\text{Road Load}} + \underbrace{M \frac{dV}{dt}}_{\text{Inertia}} + \underbrace{Mg \sin \theta}_{\text{Grade}} ,$$

where F_{TR} is the tractive force, R the tire rolling resistance, D the aerodynamic drag, M the vehicle mass, g the acceleration of gravity, and θ the inclination angle of the road.

The corresponding tractive power is

$$P_{TR} = F_{TR} V,$$

and the tractive energy required for propulsion during any given driving period is

$$E_{TR} = \int_0^T P_{TR} \, dt$$

for positive values of the integrand. The main reason that fuel is consumed in an automobile is to provide this tractive energy.

Writing an equation for instantaneous fuel consumption, integrating it

over a total driving duration, and using the mean-value theorem to introduce appropriate averages for some of the integrands, the following fundamental equation for the average fuel-consumed-per-unit-distance-traveled, $\tilde{g}$, can be obtained (Sovran 1983):

$$\tilde{g} = \underbrace{\frac{k}{\eta_b \eta_d S} [E_{TR} + E_{ACC}]}_{\substack{\text{propulsion} \\ (P_{TR} > 0)}} + \underbrace{g_u}_{\substack{\text{braking and} \\ \text{idle} (P_{TR} \leq 0)}} ,$$

where k is a fuel-dependent constant, η_b is the average engine efficiency during propulsion, η_d is the average drivetrain efficiency, S is the total distance traveled, E_{ACC} is the energy required by vehicle accessories, and g_u is the fuel consumption during idling and braking. Typical units are gallons per mile in the U.S. and liters per 100 kilometers in Europe.

Aerodynamic drag is responsible for part of E_{TR}. However, E_{TR} is only part of the propulsive fuel consumption which is only part of the total fuel consumption. The impact of drag on total vehicle fuel consumption therefore depends on the relative magnitudes of these contributions.

For the U.S. driving schedules, E_{TR} can be described accurately (Sovran & Bohn 1981) by linear equations of the form

$$\frac{E_{TR}}{S} = [\underbrace{\alpha r_0}_{\text{Tire}} + \underbrace{\gamma}_{\text{Inertia}}] M + \underbrace{\beta (C_D A)}_{\text{Aero}} ,$$

where the vehicle descriptors M, C_D, A, and r_0 are the mass, drag coefficient, frontal area, and tire-rolling-resistance coefficient, respectively, and α, β, and γ are known constants which are different for each schedule. For a typical mid-size American car, drag is responsible for 18% of E_{TR} on the Urban schedule and 51% on the Highway.

The energy part (square brackets) of the propulsion term in the fuel-consumption equation is dominated by E_{TR}, which contributes $\simeq 94\%$ for both Urban and Highway for the midsize car. The propulsion term itself accounts for $\simeq 81\%$ of the total fuel consumption on the Urban schedule and $\simeq 96\%$ on the Highway.

These quantifications permit the influence coefficient relating a percentage change in $C_D A$ to a percentage change in $\tilde{g}$ to be established. In general, this coefficient is vehicle as well as driving-schedule dependent (Sovran 1983), but for the midsize car being considered they are $\simeq 0.14$ and $\simeq 0.46$ for Urban and Highway, respectively. For the Euromix cycle, a typical influence coefficient for cars powered by spark-ignition engines is $\simeq 0.3$, while for diesel engines it is $\simeq 0.4$ (Emmelmann 1987b). In all cases, these values presume that the drivetrain gearing is rematched so

that the road load power-requirement curve runs through the engine's brake-specific-fuel-consumption map in the same manner at the lower drag as at the higher drag.

If no other changes are made in a vehicle, the benefits of reduced drag are actually threefold: reduced fuel consumption, increased acceleration capability, and increased top speed. When maximum fuel-economy benefit is the objective the increased acceleration and top-speed capabilities can be converted to additional reductions in fuel consumption. Conversion of the increased acceleration capability is accomplished by regearing the drivetrain, as discussed above. Conversion of the increased top speed requires a reduction in installed engine power, and a corresponding percentage reduction in vehicle mass so that the acceleration capability of the vehicle is not diminished.

The preceding discussions have presumed the absence of ambient wind while driving. In the presence of wind a vehicle's wind speed is generally different than its ground speed, and its yaw angle is generally not zero. This affects the operating drag force, and therefore vehicle fuel economy (Sovran 1984). On the average, the result is a reduction in fuel economy.

3.2   Handling

While traveling along a road, a vehicle experiences more than just drag. The resultant aerodynamic force has components in all six degrees of freedom (Figure 8). In principle, they all influence a vehicle's dynamics. Traditionally, test engineers distinguish between a vehicle's behavior in still
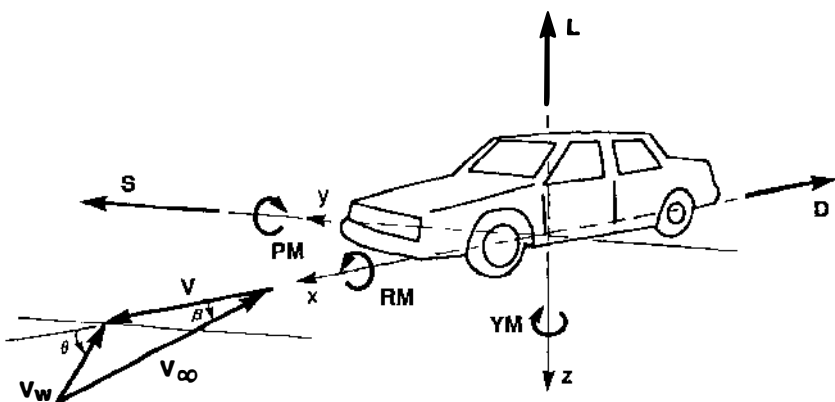

Figure 8   Aerodynamic forces and moments acting on a vehicle. Definitions of yaw angle β and the coordinate system; the latter is different from that used for flight dynamics.

air (handling), and its behavior in the presence of a crosswind (crosswind
sensitivity).

The flow over a vehicle moving through still air is nominally symmetric
about the vehicle's plane of symmetry. Lift, pitching moment and, of
course, drag are therefore the only aerodynamic components. Unless
special measures are taken, the vertical force on a bluff body close to the
ground is positive, i.e. it tends to lift the vehicle. The accompanying
reduction in load on the tires is, in principle, disadvantageous to handling.
This is because the maximum side force that a tire can generate decreases
when wheel load is reduced. However, the effect is negligible for most
vehicles except race cars—at least at reasonable driving speeds. For a
typical European car with a typical lift coefficient of 0.3, lift amounts to
less than 3% of the vehicle's weight at a speed of 60 mph, and only 10%
at 120 mph.

It is the pitching moment rather than total lift that counts in vehicle
dynamics because it changes the load distribution between the front and
rear axles, which alters the steering properties of a vehicle. With increasing
speed, a negative (nose down) pitching moment promotes a tendency to
oversteer, which is undesirable. But, this effect is hardly noticeable to the
average driver. Nevertheless some European manufacturers design their
cars for as low a rear-axle lift as possible, even if it involves a drag penalty.

In contrast, race cars live on negative lift. Their cornering capability has
been improved dramatically by aerodynamic downforce. This downforce
has to be balanced against the accompanying increase in drag, with the
nature of the balance depending on the racetrack. High-speed courses with
only a few bends, like LeMans (France), call for cars with low drag because
top speed and fuel economy are decisive (the latter determines the number
of fuel stops); speed while cornering is less important. On the other hand,
courses with numerous bends, like Brands Hatch (Great Britain), require
high downforce (Flegl & Rauser 1992) for short lap times.

3.3   Crosswind Sensitivity

In a crosswind, and while passing another vehicle in still air, the flow
around a vehicle becomes asymmetric and so a side force, a yawing
moment, and a rolling moment are produced. Also, the components of
drag, lift, and pitching moment are altered, and normally they are
increased. From both experience and numerical simulations of vehicle
dynamics, it is known that only two of these components are significant
to a vehicle's behavior in crosswind; these are yawing moment and side
force.

The yawing moment referred to a vehicle's center of gravity gives a first
indication of sensitivity to crosswind. For almost any vehicle, the yawing

moment is unstable, i.e. it tends to twist the vehicle further away from the wind. As a result, the angle of yaw, the yawing moment, and the side force are increased even further.

In recent years, the center of gravity of passenger cars has, on average, moved steadily forward. This is mainly for two reasons. First, rear-engine cars have become rare; second, the move to front-wheel drive has resulted in vertical load being shifted from the rear to the front axle. Consequently, while the yawing moment referred to the center of the wheelbase has remained relatively constant, that referred to the center of gravity has decreased. As a result, the matter of crosswind sensitivity seems to have ceased to be of concern to the driving public.

Nevertheless, crosswind sensitivity remains a subject for research. Concern is focused on the influence of the various aerodynamic and vehicle parameters on a driver's reaction in sudden crosswind gusts (Sorgatz & Buchheim 1982). Driving simulators allow for changing all these parameters independently of each other (Willumeit et al 1991). On-road driving, computations, and tests on the simulator have all led to a result which is important for aerodynamic development: Yawing moment is more disturbing than side force.

There are two reasons why crosswind sensitivity might require future attention in production vehicles: decreasing vehicle weight and increasing yaw moment. Currently, the weight of passenger cars is increasing rather than decreasing. But new government regulations on fuel economy and emissions will soon force vehicle engineers to build lighter cars, because this makes significant improvements in fuel economy possible (Piech 1992). With regard to yawing moment, it is increased by the rounded rear-end shape which is in fashion at the present time, and it will go up even further unless countermeasures are taken.

In principle, with active kinematics for the rear axle (Donges et al 1990) the twist induced by crosswind can be compensated by an appropriate steering angle of the rear wheels; this would produce dynamic stability.

3.4 Functionals

The flow over a vehicle not only produces aerodynamic forces and moments, but also many other effects that can be summarized under the term *functionals*. During the development of a new vehicle they require at least the same attention as the forces and moments. These functional effects are:

FORCES ON BODY PARTS Vehicle bodies are made up of large and comparatively flat panels, and these have to withstand considerable aerodynamic loading. Hoods, doors, and frameless windows have to be tight

under all conditions. Modern lightweight structures are prone to flutter. Special attention has to be paid to add-on parts like air shields and the various types of spoilers.

WIND NOISE   The more that the formerly dominant noise sources (i.e. engine and tires) have been attenuated, the more that wind noise has become objectionable inside vehicles. Passenger cars and buses are of particular concern. In 1983, the vehicle speed at which wind noise was of the same annoyance as the noise from those other sources was 100 mph (Buchheim et al 1983); in 1992 it is only 60 mph. Open sun roofs and side windows can also cause low-frequency noise (booming) which is extremely annoying.

BODY-SURFACE WATER FLOW AND SOILING   Water flow on a body's surfaces can impede visibility. Water streaks and droplets accumulating on the forward side windows prevent a clear view into the outside rearview mirrors. Soil diminishes the function of headlights and taillights. The sides of vans and buses are often used for advertising purposes and therefore need to be kept clean.

INTERIOR FLOW SYSTEMS   Several interior flow systems pass through a vehicle. For passenger and sports cars the design of engine-cooling ducting has become extremely difficult because of increased engine power and less underhood space. Race cars are the most demanding. According to Flegl & Rauser (1992) up to 12 separate flow ducts have to be provided; these are for the "air box" which conducts the combustion air to the engine, several coolers for water, oil, and the turbocharged air, brake cooling, and cockpit ventilation. Passenger vehicles require ducting for proper ventilation and heating of the passenger compartment. Buses require high rates of air exchange free of drafts.

4.   AERODYNAMIC CHARACTERISTICS

4.1   *Drag*

The physics of drag can be addressed from two different perspectives: 1. from that of the vehicle; 2. from that of the fluid
From Newton's third law, the forces on the body and on the stream are equal and opposite to each other.

VEHICLE PERSPECTIVE   The drag that a fluid stream exerts on a vehicle is the integral, over all surfaces exposed to the stream, of the local streamwise component of the normal (pressure) and tangential (skin friction) surface forces, i.e. $D = D_p + D_f$. The physics of drag is in the pressure (D_p) and friction (D_f) components. Measurement of only total drag (D) per se

does not provide information on their relative magnitudes, nor on their distributions over the body surfaces. However, a degree of understanding of the origin and nature of drag contributions can be and has been gained by making systematic, parametric changes in the body surfaces. This has even been accomplished in the course of normal vehicle development (e.g. detail optimization, Section 5.1).

Direct evaluation of D_p and D_f requires knowledge of the detailed stress distributions over all vehicle surfaces. To obtain this experimentally is very difficult, except for very simple shapes, even in a reasearch sense. However, direct evaluations of components of D_p have been made in selected regions of a body. This is feasible in regions where the surface pressure is reasonably uniform, e.g. in base regions where the flow is fully separated. In general, however, the direct evaluation of D_p and D_f for bodies with the complex geometries of typical road vehicles is not practical. On the other hand, detailed surface-stress distributions are the specific output of computational fluid dynamics (CFD). Adequately validated computational codes can therefore contribute greatly to better understanding of road-vehicle aerodynamics.

STREAM PERSPECTIVE   The wind-axis drag acting on a vehicle can be determined by applying the streamwise momentum equation to a large control volume containing the vehicle. One of the most significant results of the past 20 years of R&D in vehicle aerodynamics has been the identification of streamwise trailing vortices as a dominant feature of wakes. These originate in a number of different regions on a car body, and from the fluid-stream perspective are the producers (or the consequences?) of drag. In recognition of this, the momentum equation can be written in a form that expresses drag in terms of three integrals across the fluid stream downstream of the body: the downstream defects in stagnation pressure and streamwise dynamic head, and the dynamic head of the crossflow velocities in the wake which can be interpreted as a vortex drag. With uniform swirl-free inlet flow (characterized by V_∞ and $p_{t,\infty}$),

$$D = \int\!\!\int_A (p_{t,\infty} - p_t)\,da + \frac{\rho}{2} \int\!\!\int_A (U^2 - u^2)\,da + \frac{\rho}{2} \int\!\!\int_A (v^2 + w^2)\,da,$$

where u, v, and w are the local x, y, and z velocity components, respectively, in the downstream cross-section, and p_t the corresponding stagnation (total) pressure.

This method of drag evaluation and breakdown requires data from extensive and detailed traverses behind vehicles. By reducing the crossflow velocities to a vorticity field, vortex structures are better discriminated, facilitating the process of tracking them back to their origin. The method

is used primarily in research (e.g. Ahmed 1981, Ahmed et al 1984, Bearman 1984, Onorato et al 1984, Hackett & Sugavanam 1984). However, it has also been reduced to a fairly routine test procedure in one particular automotive tunnel (Cogotti 1987, 1989), where it is used as an aid in car-shape development. With it, the vortical structures in the wake are identified and their drag contributions evaluated. By tracing them back to their origin, local body-shape modifications can be explored for reducing drag. An inherent premise of this approach is that drag is minimized by minimizing vortex drag.

VORTEX DRAG   In the early years of vehicle aerodynamics the direct application of concepts and knowledge from the aircraft field seemed reasonable, and this tendency has persisted even to this day (although not usually with practicing vehicle aerodynamicists). The wing that makes flight possible is a lifting body, streamlined (i.e. without extensive flow separation), and of large aspect ratio (i.e. with nominally 2-D flow, but with 3-D end effects). Conceptual models such as circulation and induced drag have proved to be very useful for it. On the other hand, the typical road vehicle is not designed to produce lift, is bluff (i.e. has regions of locally separated flow and a large wake), and is of very small aspect ratio in planview (width/length $\simeq 1/3$ for cars). Consequently, its flow field is highly 3-D (nearly all end effect), not a perturbation of a nominally 2-D one. The concepts of circulation and induced drag (i.e. a drag component related to lift) are therefore in question for such flows (e.g. Jones 1978, Hucho 1978). Nevertheless, airfoil thinking is still used (although not usually by workers in the automobile industry) to suggest that the inadvertent lift of passenger cars produces an induced-drag component.

Trailing streamwise vortices are generated at the tips of wings by the pressure difference between pressure and suction surfaces that produces lift (Figure 9a, where a wing is represented by a flat plate with an automobile-like aspect ratio of 1/3 at an angle of attack). The strength of these vortices is lift dependent. If two identical such wings at equal and opposite angles of attack are connected together (Figure 9b) each generates tip vortices, but the net lift of the system is zero. The drag represented by the vortices is clearly not related to net lift. However, identifiable lifting-body components exist, so the vortex-related drag can be attributed to the lift of the individual wings.

Trailing vortices can also be generated by nonlifting solid bodies at zero angle of attack (Figure 9c and 9d). They are generated by local pressure gradients at edges that are oblique to the local flow. The net lift is zero and there are no identifiable lifting-body components, so the drag associated with these vortices cannot be related to a lift. This demonstrates that
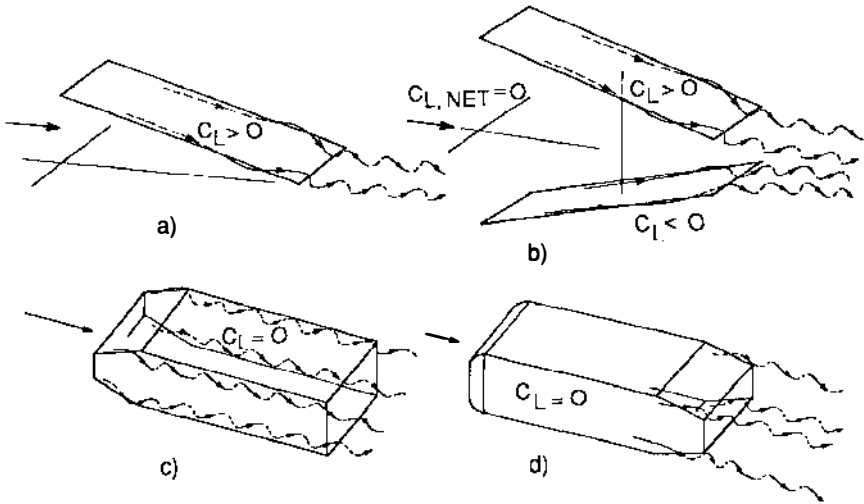
Figure 9   Longitudinal streamwise vortices (schematic) generated by lifting and nonlifting bodies.

the induced-drag concept for the contribution of trailing vortices to drag is not universal. The geometries and vortices of Figures 9c and 9d are typical of road vehicles.

CRITICAL AFTERBODY GEOMETRY   The flow over the front part of any body moving subsonically through the air is easier to manage than that over the rear. This is especially true for automobiles now that free-standing headlights, radiators, and fenders are no longer in fashion. For any current car that has received aerodynamic attention, the contribution of the fore-body to drag is usually small. This does not even require streamline shaping, just careful attention to detail. The major aerodynamic problem is at the rear.

The flow over and from the upper-rear surface of vehicles is particularly interesting. The influence of the slant angle of this surface on drag has been extensively investigated over the past 20 years (e.g. Janssen & Hucho 1975; Morel 1978a,b; Ahmed 1984). The nature of the flow behavior is illustrated in Figure 10, where the slant angle is that measured from the horizontal. As the rear roof of the simple body is slanted from the square-back baseline (point A, Figure 10a), trailing vortices are formed at its lateral edges which are drag producing. However, the downwash generated between them promotes attached flow on the central portion of the slanted surface, generating a pressure recovery that is drag reducing. The net effect is a drag reduction.
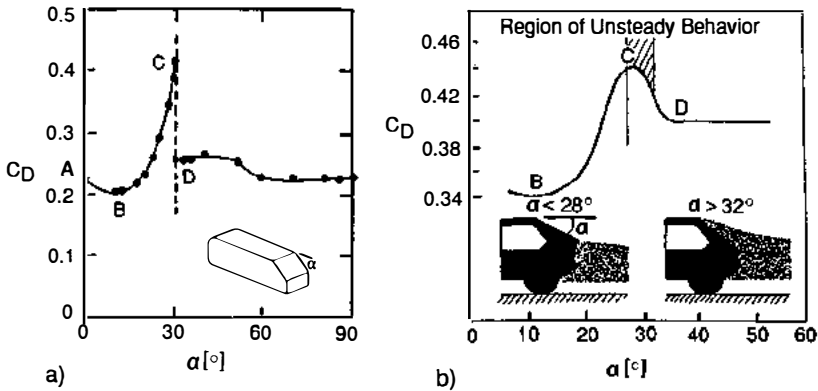
Figure 10 Dependence of drag, C_D, on the slant angle α of the upper-rear surface of fastbacks, and the existence of a critical phenomenon; (*a*) simple body, (*b*) automobile.

As the angle continues to increase the competing mechanisms grow individually, and the net drag reaches a minimum at $\simeq 15°$ (point B). It is to be noted that vortex drag is not a minimum at this point. At a sufficiently larger angle the drag reduction has decreased to zero, and further increases in angle result in a net increase in drag even though nominally attached flow is maintained on the centerline of the slanted surface.

At point C the drag is a maximum, and the trailing vortices are of maximum strength. At a slightly greater angle (the critical angle) the vortices lift off and/or burst, and the induced downwash is no longer able to produce attached flow on the centerline. The flow detaches abruptly, and a fully-separated flow develops on the slanted surface (point D). Its drag level is comparable to that of the initial square-back configuration. For this simple body with sharp rear edges, the transition is discontinuous and unidirectional. The flow patterns corresponding to C and D have been measured, and that of C is shown in Figure 11 (Ahmed 1984).

The same general behavior is observed for an actual automobile, where it was originally discovered (Figure 10b, Janssen & Hucho 1975). This has rounded edges in the slanted-roof area, and the flow pattern at transition can be bistable, switching slowly (with a period of many seconds) and randomly between that of C and D. As the slant angle increases the bistability eventually disappears, and only the D-pattern persists. For angles greater than this, the drag of the D-pattern is relatively insensitive to angle.

A drag maximum as a function of rear-upper-body geometry has also been observed for notchback cars (e.g. Figure 12, Nouzawa et al 1990). The relevant characteristic angle (β) is that between the horizontal and the
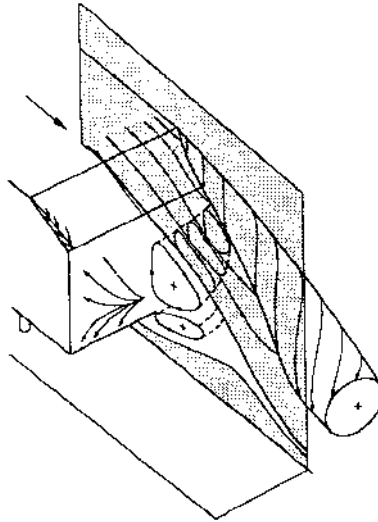
Figure 11   Wake flow pattern for a large subcritical upper-rear slant angle of fastbacks.

line connecting the end of the roof to the end of the trunk deck. For rear-window angles (α) that are $\geq 25°$, a drag maximum occurs at $\beta \simeq 25°$. At this maximum the wake pattern consists of a separation bubble behind the rear window, and trailing vortices. Measurements of instantaneous
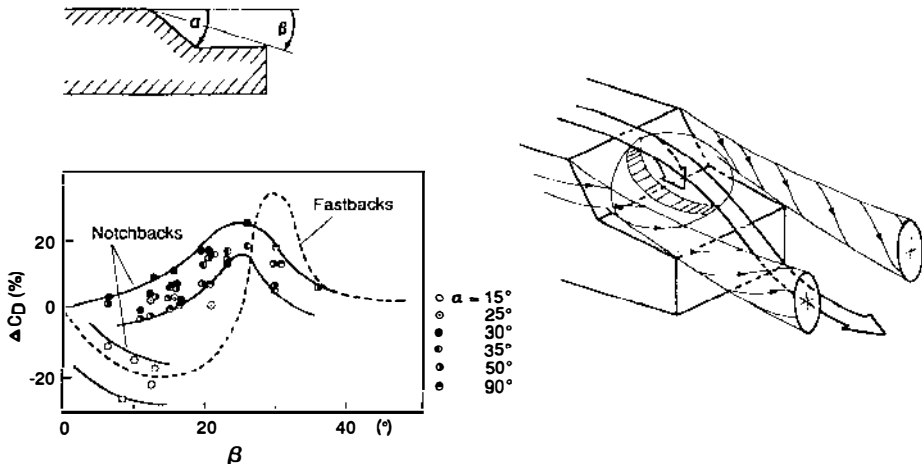

Figure 12   Dependence of drag on the afterbody geometry of notchbacks, and the wake flow pattern for high subcritical drag.

velocity in the wake and pressure on the trunk deck indicate significant bubble and wake unsteadiness (Nouzawa et al 1992). Corresponding measurements of the instantaneous drag force show that its fluctuations correlate with the unsteadiness of the separation bubble.

In vehicle design, the generic type of rear geometry (i.e. squareback, fastback, or notchback) is selected by the stylist, not the aerodynamicist. The choice is based on function and design theme, as well as aesthetics. The role of the aerodynamicist is to achieve low drag for the configuration that has been selected.

EFFECT OF AMBIENT WIND   On the average, there is always an ambient wind and the wind is not aligned with the road along which a vehicle is traveling. Therefore, road vehicles operate at a nonzero angle of yaw, on the average (Figure 13). It is the aerodynamic-force component along the direction of travel that resists vehicle motion, so this is the relevant drag. This is in the body-axis frame of reference (when a vehicle is at zero pitch angle). Some typical variations of C_D with yaw angle are shown in Figure

V ~ vehicle speed
V_W ~ wind speed
V_∞ ~ air speed
θ ~ wind angle
ψ ~ yaw angle
S_W ~ wind-axis side force
D_W ~ wind-axis drag force
D ~ body-axis drag force

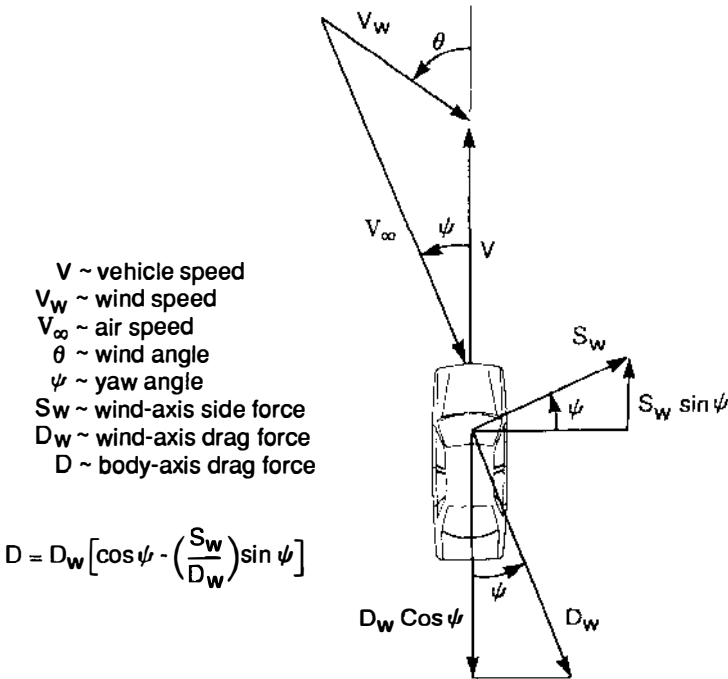$$D = D_W \left[\cos\psi - \left(\frac{S_W}{D_W}\right)\sin\psi \right]$$

Figure 13   Body-axis drag at nonzero yaw angle.

14. Driving conditions with ψ large enough to reach maximum C_D are rare, except in gusts, and average values of ψ are said to be less than $10°$ for typical driving.

As is shown in Figure 13, the aerodynamics is in the wind-axis reference frame. The variation of body-axis drag (D) with yaw angle depends on the rate of increase of wind-axis drag (D_w) and the rate of decrease of the bracketed term containing the wind-axis ratio of side force to drag (S_w/D_w). Interpreting the plan view of the vehicle as the cross-section of a bluff airfoil, this ratio is analogous to the lift/drag ratio of an airfoil. The larger S_w/D_w, the greater the rate of decrease of the bracketed term and hence the smaller the rate of increase of C_D. In an extreme case, C_D can actually decrease with ψ, i.e. the wind can contribute an aerodynamic push. This has been accomplished with an experimental, small, commuter-type, high-fuel-economy vehicle having a truncated-airfoil planform (Retzlaff & Hertz 1990).

OTHER DRAG CONTRIBUTIONS The bodies of road vehicles are characterized by two types of open cavity that communicate freely with the external flow field. One is the engine compartment, with throughflow against internal resistances. Its drag characteristics are well understood by vehicle aerodynamicists (Wiedemann 1986). The other type consists of the wheel wells; these also contain large rotating tires that pump air. The wells contribute to drag, and the exposed wheels themselves generate bluff-body drag.

A measure of the state of the art in vehicle aerodynamics is the typical C_D of production cars. In the U.S. in 1975, this was about 0.55. Today, it is about 0.35. This large improvement reflects not only the skill of the aerodynamicists, but also the greatly increased concern about vehicle fuel
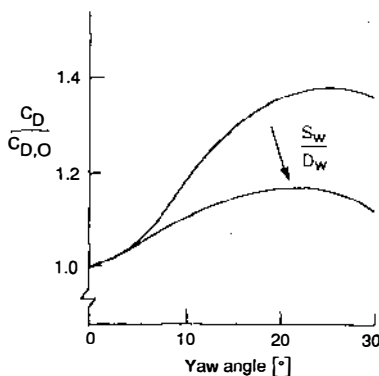

Figure 14 Typical variations of body-axis drag coefficient (normalized) with yaw angle.

economy. In Europe where fuel economy has always been important, a significant reduction in C_D has also taken place. In 1975 a typical value for production cars was 0.46. Today, several cars are below 0.30, and one car (Emmelmann et al 1990) is listed at 0.26.

4.2   Lift and Pitching Moment

The lift on a body close to the ground is determined by two counteracting effects (e.g. Stollcry & Burns 1969). Although a symmetrical body has no lift when in free air, when close to the ground the body and the ground-plane—or in the terms of potential flow, the body and its mirror image—form a narrowing channel (Venturi nozzle) between them in which the local flow is accelerated and then decelerated. This results in an average negative gauge pressure on the body's underside, tending to generate a downforce. At the same time, flow resistance in the channel displaces more flow to the upper side of the body creating an effective positive camber of the body. This makes a negative contribution to the upper-surface pressure, tending to produce an upward force.

Lift effects are pronounced on race cars, because they are generated intentionally. Two means are used to produce a large downforce.

1. A Venturi channel in the body's underside. The effectiveness of this measure is enhanced by preventing lateral flow with side skirts. A large downforce can be generated with only a small penalty in drag.
2. Negatively cambered wings at the car's front and rear, even equipped with double flaps. In this case, there is a large increase in drag due to the induced drag of the wings, and mainly from the wing at the rear (Figure 15, Rauser & Eberius 1987).

Both means for producing large downforce have been developed to such an extent that lift coefficients on the order of $C_L = -3$ have been achieved with Formula One cars (Wright 1983). This has permitted transverse accelerations beyond a driver's endurability. Therefore, in 1982 regulations prescribed only flat underbodies, and side skirts were ruled out. Now, lift coefficients on the order of $C_L = -2$ are typical, producing a downforce at 300 km/h that is approximately twice a car's weight.

To be most effective, downforce-generating elements should produce only a minimum increase in drag. One means of accomplishing this would be to make the flaps of the wings movable. In a curve, they could be deflected to a high angle to generate maximum downforce, while in the straights they could be swiveled to zero deflection for minimum drag. However, for safety reasons, movable body parts have been prohibited on race cars. A means of circumventing this regulation would be to use a jet-flap for downforce/drag control, but this has not yet been tried.
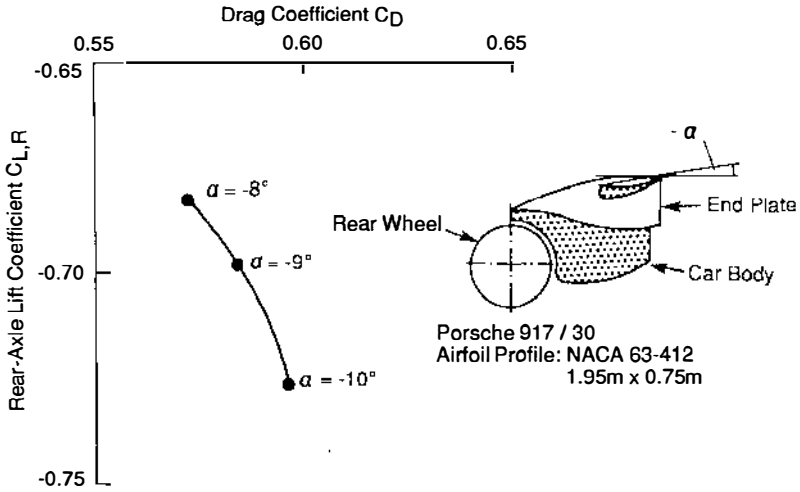
Figure 15   Rear-axle lift versus drag for three different angles of attack of the rear wing of a race car.

Passenger and sports cars use knowledge gained with race cars. Front lift is reduced by an underbody air dam; rear lift is reduced by either a rear spoiler (sometimes shaped as a wing), an underbody diffuser at the rear, or by a combination of the two. A few sports cars are equipped with a movable rear wing which is withdrawn at low speed to improve visibility to the rear.

4.3   Yawing Moment and Side Force

The generation of side force and yawing moment on cars is very much the same as the generation of lift and pitching moment on a wing at angle of attack (Figure 16, Squire & Pankhurst 1952, Barth 1960). When viewed from above, a car body can be regarded as a blunt airfoil that can generate lift (side force for the car) when its angle of attack (yaw angle for the car) is greater than zero. However, to generate a pressure diagram comparable to that for a wing the car needs a yaw angle much greater than the angle of attack required by the wing. In addition to its poor cross-sectional shape for a lifting body, this is because the aspect ratio of the car when viewed from the side (height over body length) is < 1, while that of the wing in Figure 16 is $\gg 1$. The center of pressure of the area enclosed by the pressure distributions on the lee- and windward sides is located forward of the midpoint of the car's length, and therefore a yawing moment is generated.

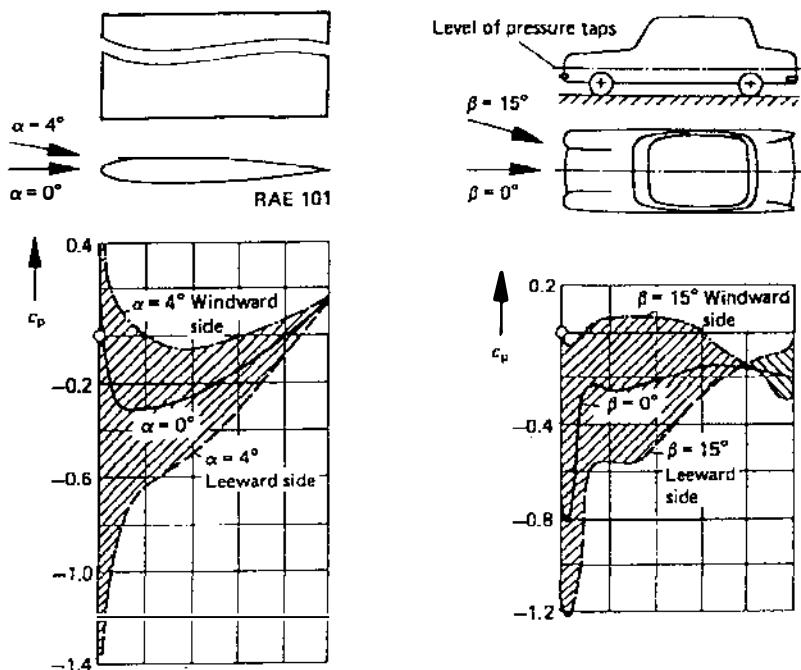Similar to airfoils, cars are aerodynamically unstable, i.e. the yawing

Figure 16 Comparison of the pressure distribution around an airfoil and a horizontal section of a car.

moment tends to turn the car away from the wind. Both their yawing moment and their side force increase almost linearly with yaw angle up to $\beta = 20°$, and side force is linear to even larger angles (Figure 17, Emmelmann 1987a). The rate of increase is mainly determined by the side-view cross-sectional shape of a vehicle. Generally, a higher yawing moment goes with a lower side force, and vice versa.

Under yawed conditions, a rolling moment is also generated, lift is increased, and pitching moment is altered. In the speed range of passenger cars, the influence of these components on vehicle dynamics is minor. However, the subjective perception of a driver has to be considered, and this is currently being investigated in a vehicle simulator.(H. Goetz, private communication).

Measures for reducing aerodynamic instability, or even reversing it to stability, have been known for a long time (Koenig-Fachsenfeld 1951). The only really effective method is the tail fin. Race cars make use of it,
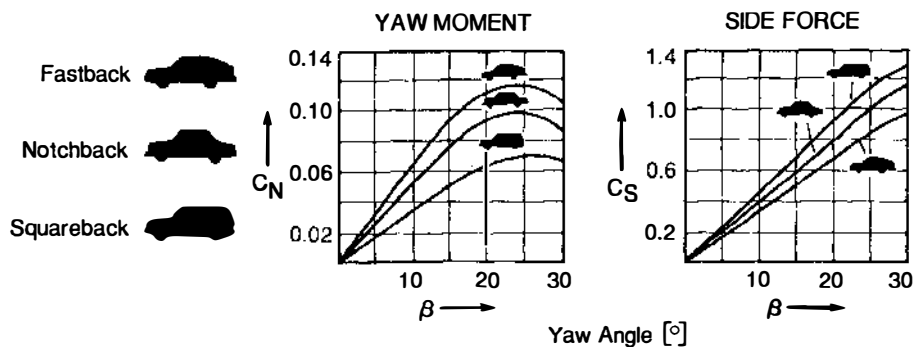
Figure 17 Yaw-moment and side-force coefficients for a family of cars with different rear-end shapes.

since the endplates of their rear wing act as such. But for passenger cars, airplane-like tail fins cannot be applied for practical reasons.

With the comparatively small shape modifications usually feasible in car development, only a limited reduction of yawing moment is possible (Sorgatz & Buchheim 1982, Gilhaus & Renn 1986). Rounded rear-end contours are unfavorable for crosswind sensitivity. Under yawed conditions the flow around the windward side's rear corner remains attached longer for a rounded corner than for a sharp edge, producing high negative pressure at this location and increased yawing moment. Some European cars have a sharp trailing edge on the rear pillars of the passenger-compartment "greenhouse" (the C pillars) to reduce yawing moment (Gilhaus & Hoffmann 1992). The accompanying increase in drag at yaw is tolerable because the large angles at which it occurs are infrequent.

Implicitly, all the preceding considerations are based on the assumption of an idealized wind, i.e. steady, with a spatially uniform velocity. In reality, this is never the case. Natural wind has a boundary layer character. When its velocity profile is combined vectorially with a vehicle's forward speed, a skewed oncoming relative-wind profile is generated (Figure 18, Hucho 1974) which cannot be reproduced either in a wind tunnel or by a side-wind facility at a test track.

Because of varying landscape along a road, the strength and local direction of wind can vary with distance along it. Furthermore, natural wind is gusty. Therefore, steady-state data obtained in test facilities cannot be exactly applicable to actual windy-day driving. The transient side force and yawing moment computed with an analytical model based on slender-body theory (Hucho & Emmelmann 1973) are significantly
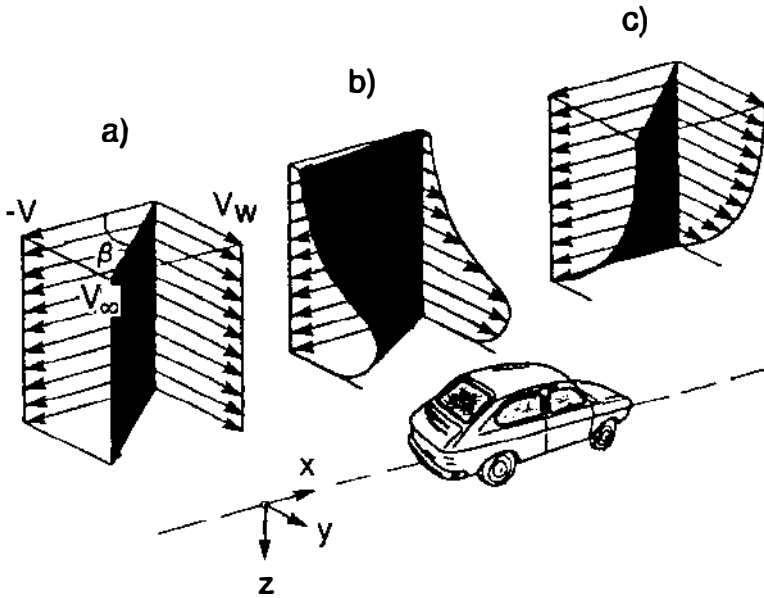
Figure 18   Wind profiles: (*a*) in the wind tunnel, (*b*) on a crosswind track, and (*c*) in natural wind.

larger than their steady state values, the magnitude of the overshoots depending on the gradient of the crosswind velocity along the direction of travel, i.e. on the gradient at the edge of the simulated wind gust.

4.4   Detailed Surface Flows

Detailed surface flows are investigated for a number of reasons: to properly locate openings for air inlets and outlets; to ascertain the forces on particular body parts; to determine the sources of wind noise; and to find means for controlling water flow and soil deposition on surfaces.

The openings for ducted air flows are placed in regions of high pressure. Therefore, the inlet for engine-cooling air has moved downward over the years along with the lower hoodlines, and is now close to the stagnation point. Consequently, large inlet grilles have become unnecessary and, to the complaint of many buyers, cars have lost their distinctive faces.

The inlet for passenger-compartment ventilation air is normally placed in the cowl area at the base of the windshield, and most commonly in the central part. The disadvantage of this location is that the ram-air volume flow rate depends on driving speed and so, therefore, does the flow velocity

inside the passenger compartment. Placing the inlet away from the center-line in an area of zero pressure coefficient avoids this speed dependency, but then a continuously running fan is needed to achieve desired interior airflow levels.

Outlet openings were formerly placed at locations of high negative surface pressure. But, due to the high flow-field velocities at such locations the local wind noise was high and was communicated to the inside of a car. Ventilation outlets are now placed in regions of low to moderate negative pressure to avoid this problem. However, the larger outlet areas required must be hidden from view; for example, behind the rear bumper.

Knowledge of the aerodynamic forces acting on body parts such as doors and the hood is needed to properly select the position of hinges and locks. Flexible structures tend to flutter, and so locations for reinforcement also have to be determined.

Wind noise, as perceived inside the passenger compartment, is receiving increasing attention. The basic phenomena are now well understood (Stapleford & Carr 1971, George 1989). However, based on buyer complaints, the application of this knowledge to specific cars still seems to be a major difficulty.

Investigations of wind noise have to deal with three factors: sources, paths, and receivers. Sources may be such things as a leaking window seal, a large-scale separation bubble on the hood, high local flow velocities, or a small-scale separation in a gap between two doors (Figure 19, Hucho 1987b). By comparing the actual flow with one where separation has been avoided by artificial means, such as by sealing door gaps, the contribution of individual noise sources can be identified (Buchheim et al 1983, Ogata et al 1987). Aerodynamic noise can also be generated by the separated flow over protuberances on a car body, such as side rearview mirrors and radio antennae (Figure 20, Ogata et al 1987). Paths have to be treated according to their function. Panels can be dampened with absorbing materials, but windows can't. Openings for ventilation must remain open. Highly turbulent separated flow from the front part of a vehicle reattaches further downstream and may excite vibrations of the structure in the reattachment area; the wake of the side-mounted rearview mirror is a typical example. The receivers are human beings. Their individual sensitivity to noise (level, spectrum, discrete tones) must be accommodated.

It might be expected that low-drag cars would produce low wind noise, but no such correlation exists for today's cars. Even aerodynamically-well-designed cars have many flow separations (of large and small scale), areas of high local velocity, and leaking seals. Further advances are needed in the ability to identify noise sources. Recent research on high-speed trains
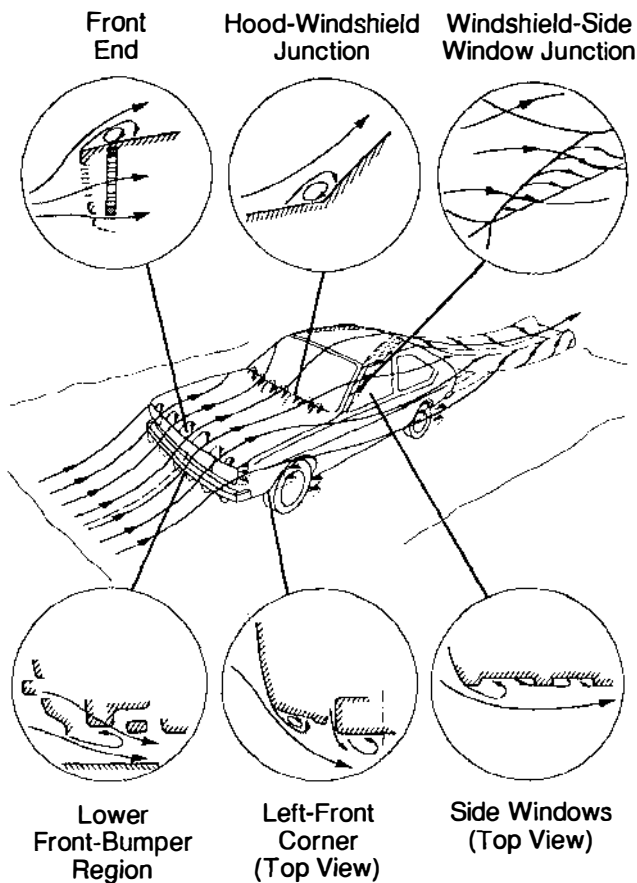
Front
End

Hood-Windshield
Junction

Windshield-Side
Window Junction

Lower
Front-Bumper
Region

Left-Front
Corner
(Top View)

Side Windows
(Top View)

Figure 19 Flow around a car, and major locations of flow separation.

(Mackrodt & Pfitzenmaier 1987) should be applicable to cars. Progress in analytical modeling of sources and paths is also a necessity (Haruna et al 1992).

The air through which a vehicle moves is not always dry and clean. Water drops (either directly from rain or from splash and spray whirled up from the road) and dirt particles (either wet or dry) are heavier than air and so do not follow streamlines. The resulting two-phase flow has to be managed with consideration for both safety and aesthetics. Two points of view deserve consideration. Whirled-up water and dirt are annoying and dangerous not only for the vehicle generating them, but also for other vehicles in its vicinity. The latter problem is still very much neglected.
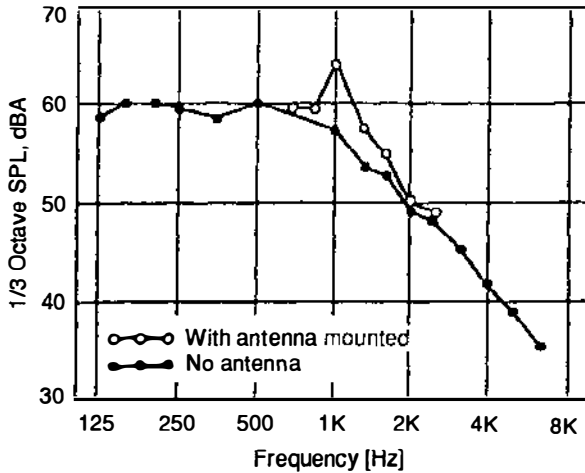
Figure 20   Aerodynamic noise generated by a radio antenna.

Water streaks that spill over from the windshield to the A-pillar (the post between windshield and front door) arc broken up into droplets by an A-pillar vortex. These droplets tend to collect on the forward part of the side windows, obscuring a driver's view in the side-mounted rearview mirrors. By integrating a rain gutter into the A-pillar, the water from the windshield can be trapped and led down and away. Similarly, water from the roof can be trapped and kept away from the rear window, either by a trapping strip in the rubber seal (Piatek 1987) or, in the case of a hatchback door, by controlling the gap between roof and door (Figure 21). If these traps are carefully faired into a body's contour, they will not cause an increase in drag.

The deposition of dirt is more difficult to prevent. Those parts of the body close to the stagnation point are the most susceptible to dirt deposition, e.g. the headlamps. Up to now, no aerodynamic alternative to the mechanical cleaning of headlamps, either by high-pressure water spraying or by brushing, has been found. Dirt deposition on the rear window of a squareback car can be reduced by a guide vane at the end of the roof. However, the air-curtain effect has to be balanced against the increase in drag that accompanies it. The sides of delivery vans can be kept free of soiling, at least partly, by impeding the dirty water that spills out of the front wheel houses. This can be achieved by generating a low pressure underneath the vehicle that reverses the direction of the wheel-house outflow from outboard to inboard.

Left Half   Right Half
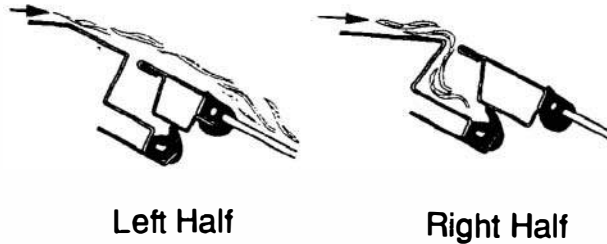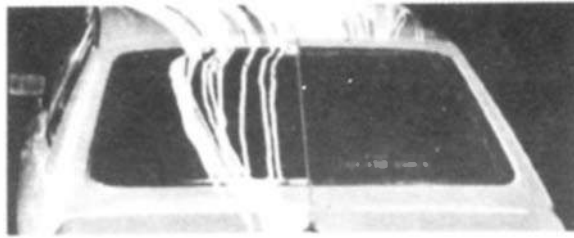
Figure 21   The gap between roof and hatch door can be used as a water trap. On the left side the large trapping gap has been sealed for the photograph, on the right side it is open and functional.

Splash and spray whirl-up is also a safety hazard for other vehicles. This is especially true for trucks and should no longer be ignored, particularly since solutions are already on hand. On wet roads, trucks with their almost uncovered wheels can raise opaque curtains of water higher than the eye-point of a neighboring car's driver (Figure 22, Goehring & Kraemer 1987). Up to now, the only way to impede this has been to completely cover all nonsteering wheels. This measure is even rewarded with a drag reduction, mainly under crosswind conditions, and is also useful in preventing cars from going under the truck in a crash.

Figure 22   Splash and spray can be kept under a vehicle by shielding the non-steered wheels. (*Left*) Wheels uncovered; the passing car can hardly be seen. (*Right*) Wheels and sides shielded, as well as the rear of the truck. (Photos courtesy of Mercedes-Benz.)

4.5 Internal Flow Systems

The flows in internal and recessed cavities that communicate freely with the external flow contribute to drag and have been discussed in Section 4.1. The flow in the passenger compartment does not make a significant drag contribution, but it has to be carefully designed for passenger comfort. High air-exchange rates have to be realized, but with a flow free from drafts. Consequently, flow velocities are kept low. The influence of buoyancy has to be recognized because of significant differences in temperature between heating and cooling. During heating, a temperature gradient is preferred (warm feet, cool head). During cooling, the conditioned air is directed to the face and chest. By making use of the physiological effect that a temperature lower than ambient can be simulated by blowing ambient air at moderate velocity over passengers, the use of air conditioning per se can be avoided in moderate climates (Gengenbach 1987).

5. DEVELOPMENT PROCESS AND TOOLS

5.1 Aerodynamic Development of a Vehicle

The aerodynamic development of a typical road vehicle follows a procedure different from that used for other types of fluid-dynamic machines, e.g. aircraft, compressors, or turbines. While the latter are designed to meet specific aerodynamic performance criteria—otherwise they wouldn't work—the aerodynamic properties of a road vehicle are largely by-products of the design process.

The typical design of a fluid-dynamic machine is accomplished in three major steps:

1. The main overall dimensions of the machine, be it the planform and span of an aircraft wing or the diameter and number of stages of a turbine or compressor, are determined by using nondimensional coefficients (derived from similarity laws) for which optimum values are known from accumulated experience. Typical coefficients are ones such as the lift coefficient (C_L) of a wing during aircraft cruise, or the specific speed (N_S) of a fan.

2. The detailed design of the machine's components follows an iterative process between analytical design and experimental verification. Computational fluid dynamics (CFD) has accelerated the convergence of this process significantly; furthermore, it permits interference effects among the components to be taken into account.

3. The separately optimized components are put together in a prototype system which is then tested. If the final device is very large, this is

preceded by testing with small-scale models. When design performance targets are not achieved, modifications are made.

The development of a road vehicle is accomplished differently. Aerodynamic development is performed in a closed loop containing aesthetic, packaging, and aerodynamic considerations. Both the number of iterations necessary and the quality of the final result depend on the ability of the aerodynamicist to recognize the intentions of the exterior designer (stylist), and to find solutions within the designer's limits of acceptability—which are extremely difficult to define because of their subjective nature.

In general, the aerodynamic development of a road vehicle can proceed from two different and opposite starting points. Typically, the designer makes the first proposal for a vehicle configuration. Then the aerodynamicist tries to improve the shape, according to his goals as described in Sections 3 and 4. One strategy which has proved to be very effective is the so-called detail-optimization (Hucho et al 1976). In this approach, details like corner and edge radii, and taper or boat-tailing are modified in small increments in order to find optimum values (Figure 5). As long as the drag coefficient of vehicles was still fairly high, say $C_D = 0.40$, the modifications necessary were frequently so small that aesthetics was hardly affected (Janssen & Hucho 1975).

The opposite approach starts with a simple body of very low drag which has the desired overall dimensions of the subsequent car. This so-called basic body is modified step by step, in cooperation with the exterior designer, until a final shape materializes which has both low drag and the desired appearance. Drag-coefficients below $C_D = 0.30$ have been achieved this way (Buchheim et al 1981). This is called *shape-optimization*.

Today the actual aerodynamic development process is usually a mixture of these two extremes. The original design of the stylist is influenced by his general knowledge of vehicle aerodynamics, more or less, and the shape modifications which are eventually necessary are constrained within rather narrow limits.

5.2 *Test Facilities*

Aerodynamic development per se is done almost entirely experimentally, guided by empiricism based on the knowledge described in Section 4. The primary test facility is the wind tunnel. Water tunnels and towing tanks are sometimes also used, but only as supplements. They lend themselves to flow visualization (Williams et al 1991), and also have the capability for reproducing the relative motion between vehicle and road, including wheel rotation (Larsson et al 1989, Aoki et al 1992). However, only those towing tanks can be used which have an extremely level and smooth bottom on which the submerged test vehicle can roll.

All vehicle characteristics influenced by aerodynamics are finally evaluated on the road. This also permits tests that cannot be made in a wind tunnel, e.g. measuring a vehicle's behavior in a cross wind.

Historically, the wind tunnel testing of automobiles started with small-scale models. Scales like 1:4 or 1:5 were preferred in Europe, the somewhat larger 3/8-scale in the U.S. The advantages of small-scale testing are that the models are cheaper than full-scale ones, are easy to handle, and can be quickly modified. Furthermore, only small wind tunnels are needed, and these are more generally available and can be rented at moderate cost.

For two reasons, small-scale testing was eventually only rarely used. At first, this was because test results from partial-scale models very often did not reproduce full-scale values with the accuracy needed. This deficiency was partly due to a lack of geometric similarity in the models, and partly to the unpredictable effects of Reynolds number. However, geometric similarity is not a fundamental problem but rather a matter of the skill and care of the model maker. Also, a Reynolds-number gap on the order of two can be bridged by artificially increasing the turbulence level of the wind tunnel (Wiedemann & Ewald 1989). Consequently, small-scale testing has again come into favor and is used by some car manufacturers with great success.

The second and even stronger objection to small-scale testing is non-aerodynamic in nature. Vehicle exterior design is done in full scale, because shapes in small scale cannot be adequately assessed aesthetically. Therefore, a full-scale model always exists, and if it is built on a realistic chassis, such as the one from the preceding model year, it can also be used as the wind-tunnel model.

5.3 Limitations of Wind-Tunnel Testing

Two major limitations exist when cars are tested in tunnels. First, due to their pronounced bluntness, cars disturb the flow in the test section of a wind tunnel significantly, the situation being similar to that with aircraft models under extreme stall (e.g. fighter aircraft during combat maneuvers). Second, the relative motion between vehicle and road and the rotation of the wheels are very difficult to reproduce, and are therefore usually neglected. However, great progress has recently been made in overcoming both of these limitations.

BLOCKAGE   As a carryover from aircraft terminology, the ratio of a car's frontal area to the cross-sectional area at the tunnel-nozzle exit is called the blockage ratio. For road vehicles, this ratio can be extremely large compared to aircraft. Blockage ratios up to 20% are sometimes used. Thermal tests (e.g. engine cooling) are done with blockage ratios even

higher than this. For a long time, a blockage ratio on the order of 5% was said to be appropriate for the aerodynamic testing of cars, this figure being borrowed from aeronautical practice. For a typical car, this would lead to a test-section cross-sectional area of 40 m^2. Very few automotive wind tunnels are this large; 25 m^2 is a typical value for the wind tunnels built recently in Europe.

With regard to the boundaries of the test section airstream, two different types of configuration are used. The closed-throat test section with solid walls is preferred in the U.S. The open-throat test section with freestream boundaries is common in Europe. The latter is characterized more precisely as only three-quarters open, the remaining quarter of the boundary being the ground floor which represents the road. A third type of boundary configuration which lies between the open- and closed-throat versions is one with slotted walls. Some automotive wind tunnels in Europe use this type (Eckert et al 1990).

Testing in an open test section is affected by a body as bluff as a car in three different ways:

1. The determination of the wind speed may be in error. If the model is too close to the nozzle's exit its flow field extends upstream far enough to modify the pressure at the location of the downstream pressure taps inside the nozzle (Figure 23, Kuenstner et al 1992).
2. The flow into the collector may be disturbed if the length (L) of the test section is insufficient and the cross-sectional area (A_C) of the collector is too small compared to the nozzle's cross-sectional area (A_N) (Figure 24, v. Schultz-Hausmann & Vagt 1988).
3. The streamlines in the vicinity of a vehicle are diverted more than in an air stream of infinite cross-section. Consequently, the drag is lower. Only this effect is subject to a blockage correction, not the preceding two.

While the first two effects are now well understood, blockage corrections for the third which are generally valid for open test sections still do not exist (SAE 1990). They are often said to be small and are therefore, for simplicity, neglected. It is doubtful whether this holds for blockage ratios of 10% or more.

The effect of body bluffness on closed-throat tunnel testing is primarily one of model blockage, although a possible influence on the wind-speed measurement cannot be ignored. In contrast to open throats, the streamline divergence around a model is less than that in an infinite stream. This causes the measured values of C_D to be larger than those in an infinite stream, rather than smaller, and the magnitude of the discrepancy is significantly greater than that for open test sections.
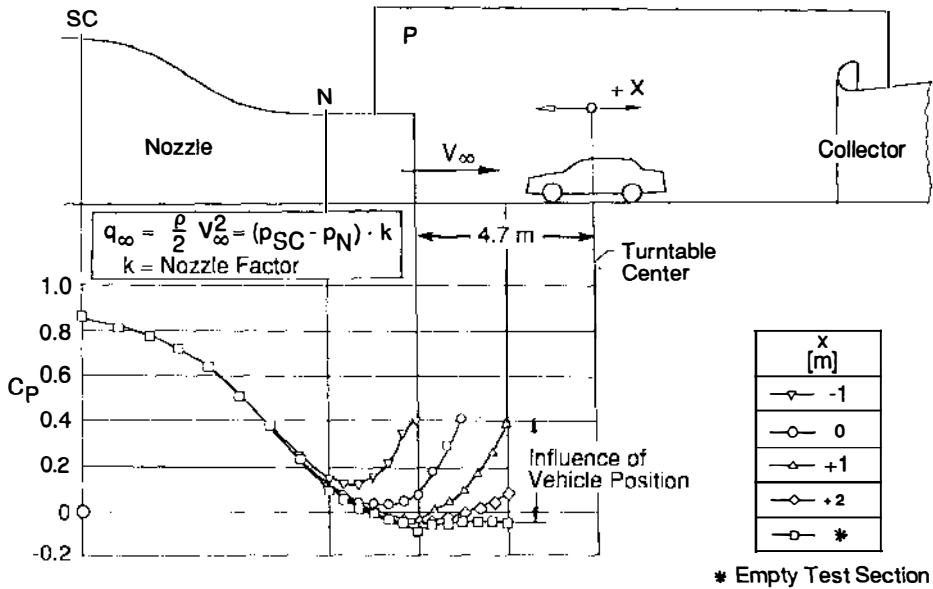
Figure 23 Pressure distribution on the centerline of the floor inside the nozzle of the BMW 10 m² acoustic wind tunnel. If the model is positioned too close to the nozzle's exit, the static pressure at location N is increased.

All classical blockage corrections are all-inclusive in nature, i.e. the velocity head of the oncoming wind is first corrected, and then the co-efficients corresponding to all the measured forces, moments, and pressures are adjusted using this corrected head. The assumption underlying any concept of data correction (it is, more properly, data adjustment) is that the detailed nature of the flow field (in a nondimensional sense) is unchanged by blockage. This does not necessarily hold if the blockage ratio is large, or if flow separations and reattachments are affected.

Blockage correction for road vehicles in closed test sections has been the subject of an ongoing cooperative study by aerodynamicists active in vehicle testing (SAE 1991). From the many procedures considered, three have been established as acceptable for zero-yaw-angle testing in this application. These are: a wall-pressure signature method (Hackett & Wilsden 1975), a less comprehensive wall-pressure method (Hensel 1951), and a semi-empirical method (Mercker 1986). All three give approximately the same blockage correction, even at nonzero yaw angle. The pressure-signature method is the most comprehensive, requires the least subjective user input, and is readily applicable to vehicles with unknown flow patterns. It has the disadvantage of being demanding in terms of instru-
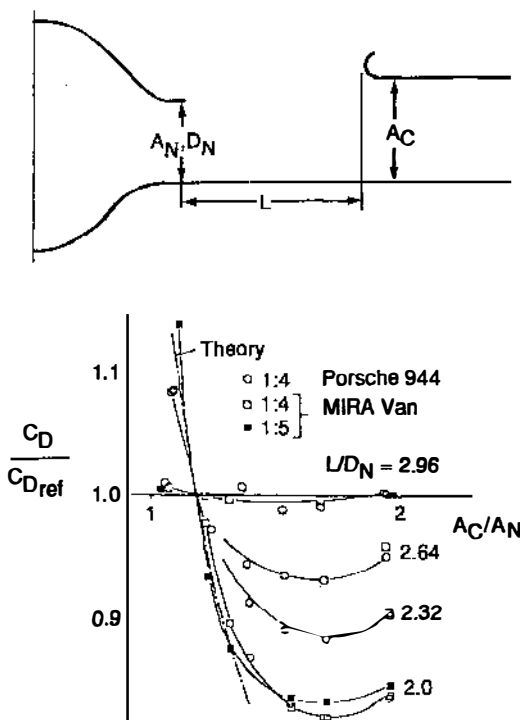
Figure 24 Influence of test-section length L (relative to the hydraulic diameter D_N of the nozzle) and the ratio of collector area (A_C) to nozzle area (A_N) on measured drag; Porsche 22 m^2 wind tunnel, open test section.

mentation and computation. The method has been modified and extended for tractor-trailer trucks by Schaub et al (1990), and the improvement is applicable to automobiles.

ROAD REPRESENTATION AND WHEEL ROTATION   From the numerous suggestions for simulating the road in a wind tunnel (Figure 25) the following four have been reduced to practice (Mercker & Wiedemann 1990): a solid floor without any boundary layer control (*a*), with tangential blowing (*h*), or with boundary layer suction, (*d* and *g*); a moving belt in combination with an upstream scoop or a suction slot to remove the oncoming boundary layer (*c*).

The simplest and most common way to represent the road is with a solid and fixed ground floor. This permits a vehicle to be easily connected to a balance under the floor through four pads, one under each wheel, which can be adjusted for wheelbase and track. The wheels of a vehicle are not rotated during conventional testing. As long as the displacement thickness
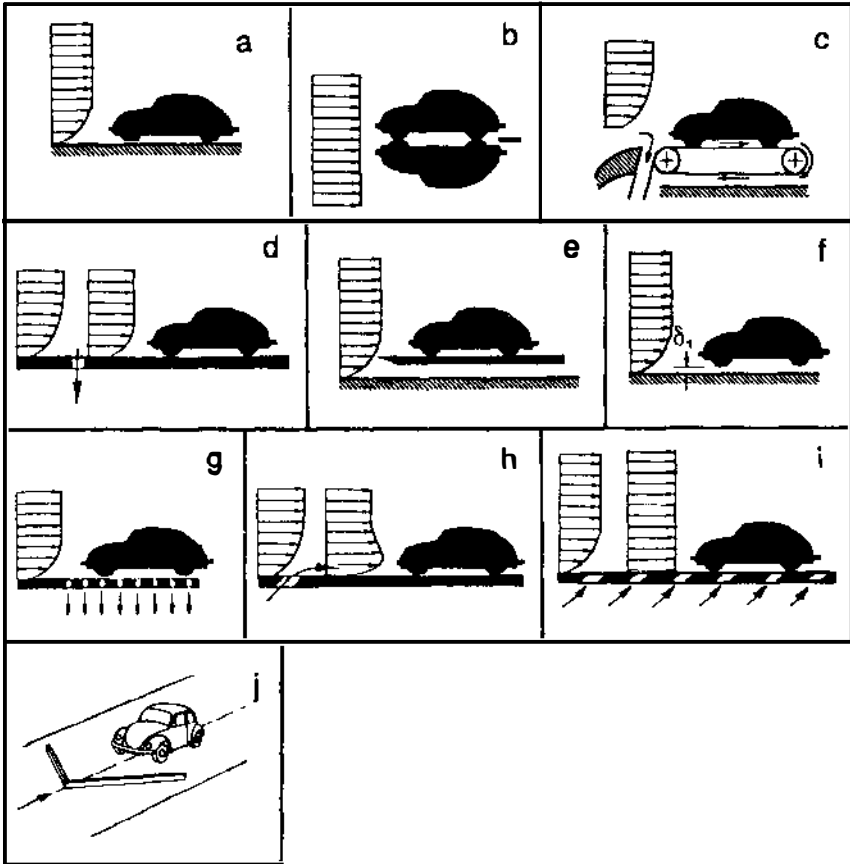
Figure 25 Various possibilities for representing the road in a wind tunnel.

of the floor boundary layer, as measured in an empty test section, is less than 10% of the vehicle's ground clearance, this kind of ground simulation is adequate for passenger-car development at drag-coefficient levels of $\simeq 0.40$ and above (Hucho et al 1975).

The moving belt represents (in principle at least) an almost perfect way to simulate the road. There are a surprising number of moving-belt wind tunnels in the world used for automotive testing. Nearly all of them (20, by one count) are for partial-scale models, and many are used for testing Formula One race cars. Quite a number are at educational institutions. There are only two full-scale facilities.

In moving-belt tunnels the belt's ability to support the weight of the test vehicle is limited. Therefore, in nearly all of them the vehicle is suspended

from a force balance located above the test section, usually by a vertical strut. This strut is shielded from aerodynamic loads by a streamlined fairing. In a very few facilities the vehicle has an internal balance and is supported from the rear by a sting. The resultant aerodynamic interference of the strut or sting can be significant, and must be quantified by calibration.

Nonrotating wheels over a moving belt require a gap bctween wheels and belt, and this leads to errors in drag and lift (Beauvais et al 1968). Consequently, in all moving-belt facilities the wheels of the test vehicle are in contact with the belt, and driven by it. While the two-fold effect increases the fidelity with which the wind tunnel simulates on-road driving, it also confounds the aerodynamic measurements. The wheels are either attached to the vehicle in a manner that prevents their vertical loads from being transmitted to the body, or detached and independently supported in a manner that permits the streamwise force on them to be measured. In either case, the lift of the wheels is not measured. Furthermore vehicle drag can be inferred only if appropriate correction is made for the rolling resistance of the tires. The latter is determined by a tare test with the belt moving but the wind off.

A means for measuring the lift of a complete vehicle (i.e. including the contributions of the wheels) as well as that of only its body has been developed for full-scale cars. The vehicle is fitted with an internal balance and supported from the rear on a sting (Figure 26, Mercker et al 1991).
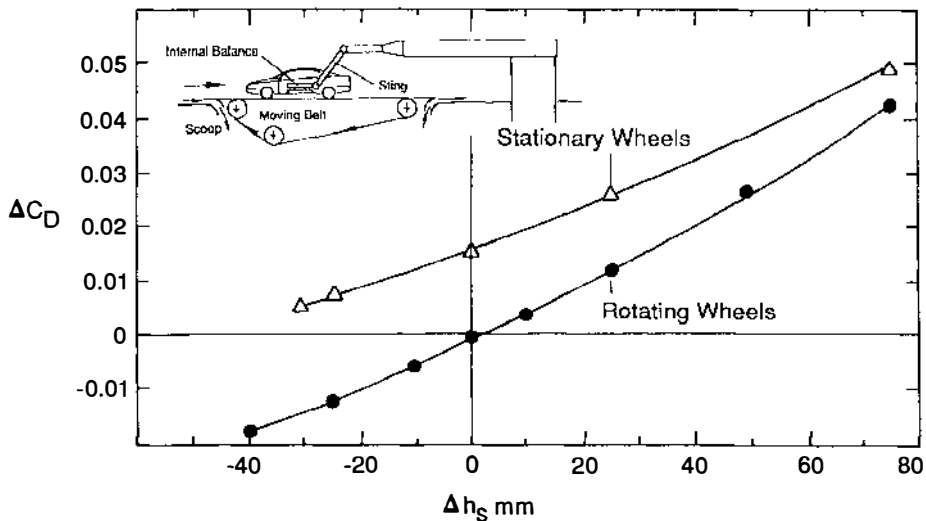

Figure 26 Influence of wheel rotation on drag, as measured for an Opel Calibra over a moving belt in the German-Dutch wind tunnel (DNW): Δh_s is the difference in underbody clearance height from the design level.

The suspension of all four wheels is replaced by a pneumatic system which permits accurate control of the vertical load at each wheel. This is necessary to permit measurement of the total vehicle lift, and to properly simulate the tire rolling resistance which depends on vertical load. The technique requires considerable model preparation, and setting up the test and performing the necessary calibrations requires much valuable time in the test section. Therefore, it is not well suited for routine testing, and is primarily restricted to research.

The influence of wheel rotation per se on the drag of passenger cars has been evaluated using this technique (Figure 26, Mercker et al 1991). Rotating wheels make a smaller contribution to vehicle drag than stationary ones. In addition, wheel rotation increases vehicle lift significantly.

It is argued that tangential blowing over a fixed floor comes close to a moving-floor simulation (Figure 27, Mercker & Knape 1989). In order to cope with wheel rotation, special wheel pads are under consideration. Either a miniature moving belt or a pair of little rollers integrated into the pads under each wheel may provide a practical solution.
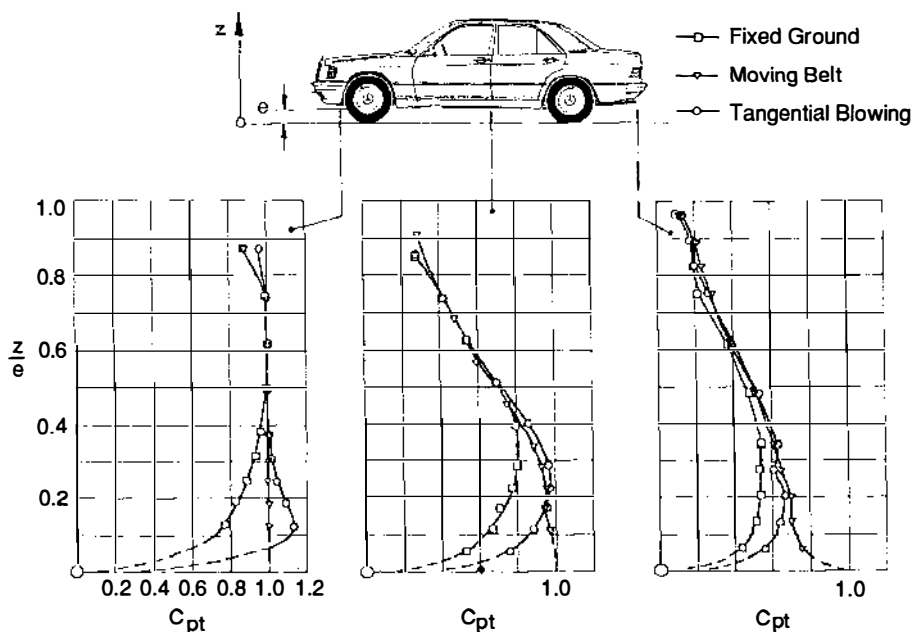

Figure 27   Dynamic-head distribution $[C_{pt} = (P_t - p_\infty)/q_\infty]$ in the centerplane under a vehicle in a wind tunnel with three different types of ground plane simulation: fixed ground, moving belt, and tangential blowing.

In some fixed-floor automotive wind tunnels, boundary layer suction is applied, most frequently as concentrated suction. Air is sucked off through a strip of perforated sheet metal at the nozzle exit. The alternative, distributed suction, is used in only one tunnel (Vagt & Wolff 1987, Eckert et al 1992). In this case air is sucked through a large porous area of the ground floor in front of and under the car. The use of several suction chambers permits spatial variation of the suction rate over the surface of the floor.

In comparison to tangential blowing, suction has several disadvantages. If the boundary layer is to be reduced by the same amount, a much larger volume of air must be removed than is added when blowing is employed. Consequently, the negative angle of attack of the oncoming flow induced by the suction may exceed a tolerable value for car tests, say 0.2°. Forces and moments on a car are very sensitive to angle of attack.

With distributed suction, it is also not clear how much air should be sucked off, nor where. In comparison to the natural floor boundary layer in an empty test section, the thickness of the boundary layer on the ground underneath a moving vehicle is small (Hucho et al 1975), but not known a priori. Therefore, it is difficult to define the proper suction rate and distribution. In the case of tangential blowing, it has been empirically determined that the blowing rate required for zero displacement thickness in an empty tunnel at the location of the front wheels of a car will result in aerodynamic measurements in good agreement with those obtained with a moving belt (Mercker & Knape 1989).

5.4   New Test Facilities

Aerodynamic noise can be investigated in a wind tunnel only if there is a sufficient difference in sound-pressure level between the noise produced by the flow around (and through) a vehicle and the background noise of the tunnel. The formerly required 10 dB(A) difference (Buchheim et al 1983) may be sufficient for objective measurement of the external sound pressure field, but it is inadequate for subjective assessment of wind noise inside a car. Aero-acoustic wind tunnels have now been built which provide a 30 dB(A) sound-pressure-level difference (Ogata et al 1987, Hucho 1989a). Existing tunnels are now being equipped with additional sound dampers, even at the expense of a lower maximum wind speed, to make them better suited for aero-acoustic investigations.

Thermal tests make up the other half of vehicle aerodynamics. Adequate comfort for passengers and proper functioning of the engine and accessories have to be guaranteed under all operating conditions. One approach to thermal testing is to perform all aerodynamic test work in the same facility (Moerchen 1968). The other is to use separate specialized facilities

for each kind of test. The latter has turned out to be the more efficient. Facilities for thermal tests can tolerate a less accurate simulation of the flow field around a car, so they can be built much smaller. Furthermore, the number of aerodynamic and thermal tests has grown so large that more than one facility is needed in any case. For air conditioning work in passenger cars, climatic tunnels with a test-section area between 6 and 10 m^2 are suitable (Buchheim et al 1986). An airstream of even smaller cross-section can be used for engine-cooling tests, and 2 to 4 m^2 are sufficient (Basshuysen et al 1989).

5.5   Measurement Techniques

The motivations for improving measurement techniques have been, and still are, threefold: time saving, increased accuracy, and more-detailed information for reaching the ever-higher aerodynamic targets.

Routinely, the frontal area of every model has to be determined. Formerly, this was done by projecting the shadow of a vehicle on a screen using a spotlight a long distance in front of it, and integrating the area of the shadow by hand. This procedure has now been replaced by several fully automated techniques using laser light (Buchheim et al 1987) which are far faster and more accurate.

For a long time, only three kinds of measurement were performed during routine vehicle-shape development: forces and moments; pressure distribution on specific sectors of the surface; and flow visualization by various techniques (Hucho & Janssen 1977). Information on the flow field was rather limited, leaving shape modification to the imagination and experience of the test engineer.

Deeper insight into flow mechanisms should provide a more rational basis for development work, but this requires additional types of data. Boundary layer profiles on the external surfaces and underhood velocity distributions are now being measured by laser-Doppler anemometry (LDA) (Buchheim et al 1987, Cogotti & Berneburg 1991). Wake surveys are being made with multi-hole probes (Cogotti 1987, 1989) and evaluated on the basis of momentum considerations (see Section 4.1).

5.6   Computational Fluid Dynamics

The primary reason for the automobile industry's interest in numerical methods is to save time during product development. The ability to quickly react to the ever-changing needs of the market has even higher priority than cost saving, which is very important in its own right. Consequently, all numerical methods need to satisfy two conditions—the first one is necessary, but only the second is sufficient:

- They have to reproduce the related physics with adequate accuracy;
- They have to be faster than experiment.

Only in some narrow niches does computational fluid dynamics as applied to vehicles fulfill both these conditions today. CFD is still more a subject of research than a development tool.

What accuracy means in this context becomes evident from the following requirement: CFD must be able to discriminate a change in drag as small as $\Delta C_D = 0.002$ (Ahmed 1992). Also, computing time has to be competitive with the wind tunnel (Hucho 1989b). The time needed to carry out one specific modification to a model and make the related measurement in a wind tunnel is only from five to ten minutes in partial scale, and from ten to fifteen minutes in full scale.

However, when it finally becomes practical, CFD will have much to offer. First of all, it can generate information before a testable model even exists. Secondly, numerical methods are not necessarily burdened with the limitations of the wind tunnel. For example, computational space can be made large enough to eliminate blockage effects, although not without cost. Also, simulation of the relative motion between vehicle and road and rotation of the wheels are comparatively easy to accommodate. Finally, once the equations have been solved, there is much more information available than from a routine experiment.

Exterior designers would be happy if reliable predictions of aerodynamic characteristics could be made right now. More and more, their creative design process is taking place on the computer. The selection of candidate designs is being made from the computer screen, and aerodynamic data (e.g. C_D) could contribute to these pre-hardware decisions, but only if CFD is able to generate results on time. Ultimately, it should only be necessary to build one or two clay models to finalize a configuration.

Consequently, a large effort is under way to improve CFD, and this is documented in numerous recent publications (e.g. Ahmed 1992, Kobayashi & Kitoh 1992). Four different routes are being followed in the application to road vehicles. They are based on:

- Laplace's equation,
- Reynolds-averaged Navier-Stokes equations (RANS),
- instantaneous Navier-Stokes equations, called direct numerical simulation (DNS),
- zonal models (hybrids).

The Laplace equation is being solved by the well-known panel method; only the surface of the model (and the road) have to be discretized. The vortex-lattice method has only been applied infrequently to cars (Stafford

1973), but was recently used to simulate the trailing vortices at their slanted base (Hummel & Ramm 1992). By definition, only nonviscous flow can be treated with the panel method, and hence no information on drag can be expected. Results are improved if the wake is modeled (Ahmed & Hucho 1977). Its geometry has to be taken from experiment, or from intuition. Pressure distribution can be predicted fairly well on all surfaces where the flow is attached. Forces and moments on body panels like doors, hood, and windows can be calculated. The panel method has been successfully applied to the development of the German high-speed train ICE (Inter City Express, Mackrodt et al 1980). The shape of the train's front end had to be designed to create the smallest possible pressure wave, in order to avoid problems when entering tunnels, passing through stations, or when two trains pass going in opposite directions.

The Reynolds-averaged Navier-Stokes equations (RANS) need a turbulence model for closure, and there is much controversy in the fluid mechanics community as to which one is the most appropriate. In engineering applications the k-ε model is the one most widely used. Close to a wall the empirical logarithmic law of the wall is usually applied, but has only been validated for plane two-dimensional boundary layers. As previously described, the flow over a road vehicle is anything but 2-D.

A very good result has been reported with the RANS concept (Hutchings & Pien 1988). Drag was predicted correctly for a generic car model; however, there were significant differences between computed and measured pressure distributions on the upper and lower rear surfaces. This highlights the need to validate more than the prediction of overall aerodynamic forces, since these might fortuitously camouflage the presence of large, but compensating, errors in local flows.

To date, none of the RANS codes has reproduced the large changes in flow pattern and drag that take place at a critical slant angle of the upper-rear surface of vehicles (see Section 4.1). A computation of such critical behavior has, however, been made using the full instantaneous Navier-Stokes equations (Figure 28, Tsuboi et al 1988). The longitudinal slender cylinder with slanted base of Morel (1978a) was used, and it was located out of ground effect. This configuration was used by Morel to explore the drastic change in drag at a slant angle of $\simeq 30°$ discovered during the development of the Volkswagen Rabbit (Figure 10b, Janssen & Hucho 1975). Numerical results (drag coefficient and flow pattern) agree well with the measurements. Whether or not all the turbulence scales at the test Reynolds number were adequately resolved with the computational grid employed is an open question.

This result has stimulated numerous applications of DNS to actual vehicle development problems in Japan. With almost 10^6 grid points for
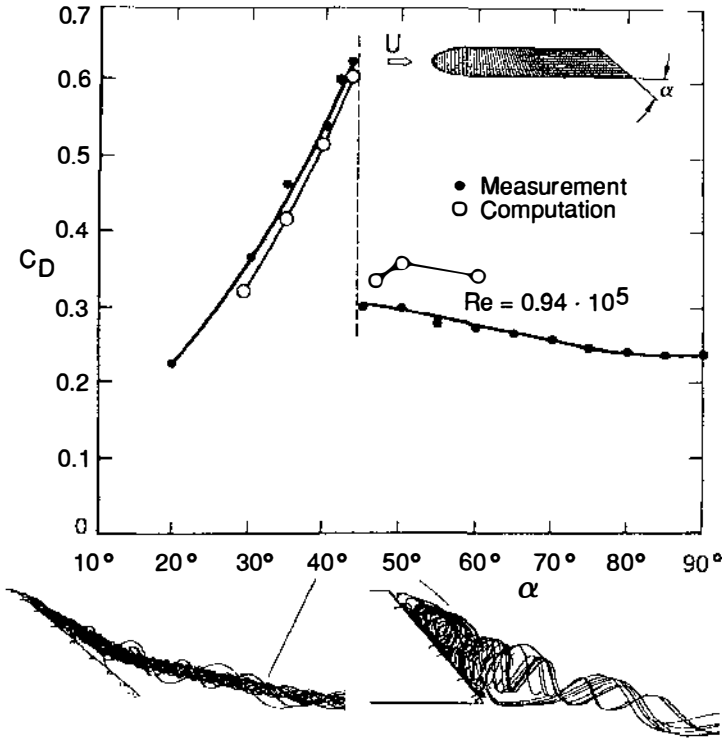
Figure 28 Drag versus rear slant angle α computed with a DNS code and compared to measurements at the same Reynolds number (measurement: Morel 1978a; computation: Tsuboi et al 1988). Bottom: computed flowpaths of the vortices emanating from the sharp edge of the slant.

a half model, DNS has been able to discriminate the effect of several aerodynamic devices (spoilers, flaps) on the drag and lift of a sports car (Figure 29, Kataoka et al 1991). Grid generation is said to require only three days, and CPU-time for a single configuration between 10 and 20 hours on a supercomputer. Calculated drag compares to measurement within 5%.

Hybrid computational schemes need some a priori knowledge of the flow field. The field around a model is partitioned (Larsson et al 1991) into zones of attached flow and zones where separation is expected to occur. The flow in the first type of zone is computed iteratively with a panel method and a boundary layer code. The second zone is treated with either RANS or DNS. An alternative approach is to compute the attached flow with an Euler code and a boundary layer code, and to model the wake.
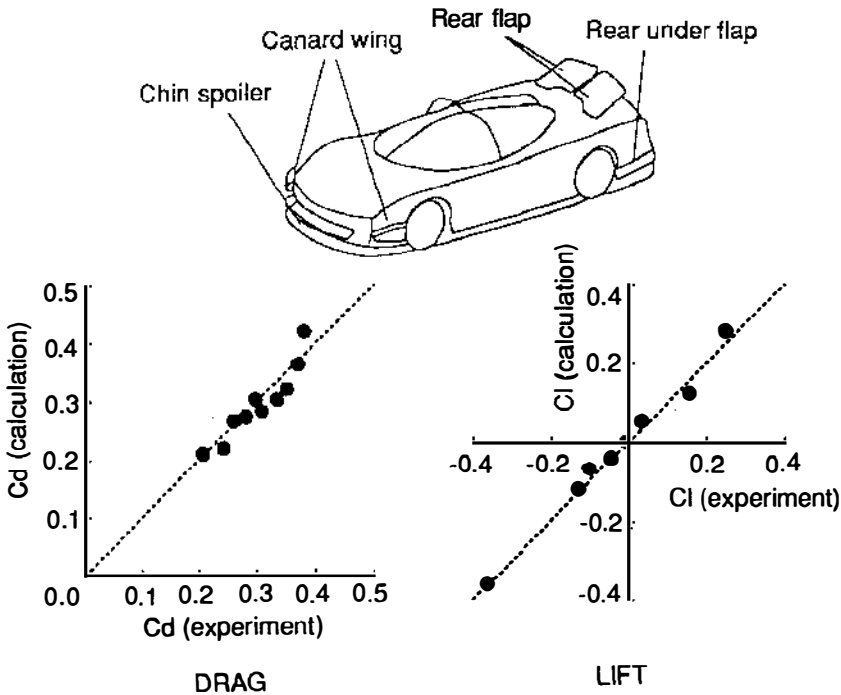
Figure 29 Comparison of computed (DNS) and measured drag and lift coefficients for a sports car with various aerodynamic devices.

Vorticity is generated within the boundary layer, and its transport can be computed with the Euler equations. A promising result has been achieved for two-dimensional flow around a circular cylinder (Krukow & Stricker 1990). No 3-D results and no details of the wake model have been published.

CFD has also been applied to internal flow systems, whose common feature is that they are nonisothermal. Underhood flow has been computed with RANS using the k-ε turbulence model (see e.g. Kuriyama 1988). Interaction between the interior and exterior flows has been treated by simultaneous computation of both flow fields (Ono et al 1992). The flow pattern inside the passenger compartment of cars and buses attracts increasing attention. For moderate air fluxes the velocities are sufficiently small that a laminar treatment is appropriate (Figure 30, Glober & Rumez 1990); for greater fluxes, turbulent flows have been computed (e.g. Ishihara et al 1991). Temperature and velocity distributions inside the compartment have been used to compute the thermal comfort of passengers, with
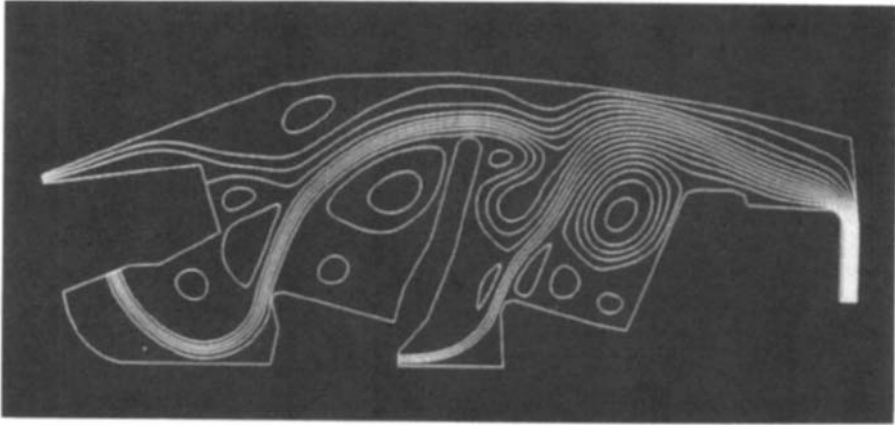
Figure 30   Streamlines inside a passenger compartment without passengers; laminar flow.

humans being described by a discretized thermo-physiological model (Dick & Stricker 1988).

CFD lends itself to the development of corrections for wind-tunnel data, but has been used for that purpose in only a few cases. However, the contours of interference-free streamline-shaped tunnel walls, either fixed (L. G. Stafford 1979, personal communication) or adjustable (Goenka 1990), have been computed. The geometries of the vehicles in the test section were comparatively simple because only their far-field flow was needed. A blockage ratio of up to 20% can be accommodated with properly shaped walls.

5.7   *Empirical Methods for Drag Estimation*

Early in the recent history of automative aerodynamics it was perceived as a shortcoming that the aerodynamic characteristics of a vehicle could only be established by measurement. The Motor Industry Research Association (MIRA) tried to overcome this with a rating method for drag (White 1967). It made use of nine descriptors of a vehicle's shape. Each geometric feature, such as the front end or the A-pillar, had to be subjectively rated with regard to its drag contribution. The drag of cars was high in those days, the coefficient ranging from 0.50 to 0.60. Freestanding headlamps and fenders were still in vogue. The method had the virtue of identifying those areas that were most important for drag, but it was unsuited for shapes with lower drag. Later, when CFD was still not recognized as being applicable to vehicle design, MIRA made a second attempt at a rating method (Carr 1987). Similar to the first one, drag is broken down according to the location of generation: forebody, afterbody, underbody, wheel and wheel wells, protuberances (e.g. mirrors), and engine cooling system. The

contribution of each of these is determined using empirical functions which correlate geometric parameters (similar to those shown in Figure 5) that can be read from a vehicle drawing with local drag. Some 50 generic details are taken into account, 27 empirical (confidential) constants are applied, and no subjective rating is required. Validation of the method with 26 cars (Rose 1984) resulted in a fairly high accuracy of $\pm 5\%$. The method could be integrated into a CAD system, but its limits of applicability are difficult to define. Also, a major drawback is its linearity: No interaction between the various regions of a car body is allowed for. Work is currently under way at MIRA to extend this rating method to lift and lateral coefficients.

An attempt to develop an expert system for drag prediction failed despite promising first results (Buchheim et al 1989), and has been abandoned.

6. OPEN ISSUES AND FUTURE TRENDS

Using drag coefficient as the measure of the state of the art in vehicle aerodynamics, further progress appears to be possible. Today, well-tuned cars have drag coefficients of about 0.30. However lower values are possible (Figure 6), and have already been realized with production cars (Emmelman et al 1990). Whether or not they are feasible for any particular car is more a question of consistency with the vehicle's design concept than it is of aerodynamic capability.

Drag will be of even greater importance for some of the specialty vehicles likely to be on the market in the future (e.g. electric, hybrid). The greatest problem of electric vehicles—limited driving range—is directly impacted by drag. Drag coefficients less than 0.20 are feasible, and electrics can provide the incentive for achieving them. However, the development process will be of increased difficulty because there appears to be significant interaction between the local flows in different areas of a car body at these low drag levels.

If future fuel economy regulation forces cars to become much lighter, the other components of the resultant aerodynamic force will become more important. Directional stability can be improved by reducing lift, mainly at the rear axle. Sensitivity to crosswinds must be kept under control by reducing yawing moment and side force.

The management of underhood airflow will become more and more difficult. Fuel economy regulation is forcing more compact body shapes, and a current styling feature is lower hood lines. Together, they are dictating smaller, and hence more tightly packed, engine compartments. At the same time, the airflow requirement is increasing. Firstly, ozone-layer depletion has mandated a worldwide elimination of the chlorofluorocarbon refrigerant (freon) currently used in automotive air con-

ditioning systems. (in 1991, $\simeq 95\%$ of the new cars sold by U.S. manufacturers had air conditioning). Its environmentally friendly replacement is a less effective refrigerant and requires more airflow for condenser cooling. Secondly, higher underhood temperatures are having a deleterious effect on the durability of engine and vehicle accessories in the engine compartment, and so these temperatures must be controlled. The combination of increased airflow requirement, higher-resistance air path, and under-bumper air inlets will make thermal management of the underhood compartment even more difficult than it is today. Consequently, it will require an even larger fraction of the aerodynamic effort expended in new-vehicle development.

Other parts of the flow field will also call for closer attention. Splash and spray have to be kept under control—not only for trucks where technically feasible solutions are waiting for application. Wind noise has to be reduced as the engine and tires become quieter.

The designers of vehicle shape need more room in which to maneuver. Sometimes they create new aesthetic shapes that are unfavorable for low drag. The required aerodynamic compensation has to come from places that do not affect appearance. Such regions are the vehicle's underside, the wheels, and the wheel wells.

From experiments in both research (Cogotti 1983) and development (Mercker et al 1991) it can be concluded that wheels and wheel wells contribute approximately half the drag of a low-drag car. Major contributors are the front wheels. Due to an outwardly spreading flow under the front part of a vehicle, the local flow approaches the front wheels at a large yaw angle, resulting in high wheel drag. Wake measurements (Cogotti 1987) also confirm this. Because cars must have wheels, and unconventional wheel arrangements are unacceptable, the only way to improve the situation is to suitably control the lateral spreading of the flow under a vehicle. However, only very modest attempts at this have been made so far (Emmelmann et al 1990).

With respect to wind-tunnel test techniques, ground simulation has to be improved for routine testing. Miniature moving belts or mini-dynos, one under each wheel, together with tangential blowing seems to be a feasible approach. Better boundary corrections (adjustments) for open-jet test sections are to be expected by using CFD.

Computer technology per se continues to improve at an almost astonishing rate. More and more aerodynamic computations (CFD) will become possible. They will definitely have a role in research. The question is the degree to which they will be feasible in vehicle development (accuracy, cost, time). How will CFD stack up against intelligent experimentation, e.g. as exemplified by the detail-optimization technique? Will it cope better

with the increasingly interactive nature of the flow fields associated with
very-low-drag shapes which is making experimental implementation of
that technique more difficult? In principle, DNS can do it all. But are
computational grids fine enough to discriminate all the scales of turbulent
flow at realistic operating Reynolds numbers possible and/or feasible?
Even if they are, is the huge amount of detailed data generated actually
needed for good aerodynamic design?

Despite some fascinating published results from CFD, the technology is
still applicable in only limited areas during the daily course of aerodynamic
engineering. From the authors' point of view, the major reservations on
existing CFD codes are that, with the exception of the panel method, their
accuracy and limits are not well known. Many published comparisons
with experiment have been made for body geometries having flows that
are too complex. Consequently, it is not possible to determine whether the
differences between experiment and CFD are due to the physics of the
equations (e.g. turbulence model), numerical characteristics (e.g. mesh
geometry, numerical algorithm, computation scheme), or a combination
of the two.

As has been common practice in other areas of fluid dynamics, com-
putational codes should be tested—and developed—by comparing their
results with either exact (analytical) solutions (which don't exist for com-
plex turbulent flows) or with experiments, but one should start with simple
flows. Only when these are fully understood is the step to more complex
flows justified. Configurations like cars and trucks have extremely complex
flow fields. They should be tackled at the end of a code development
process, not at the beginning.

Literature Cited

Ahmed, S. R. 1981. Wake structure of typi-
cal automobile shapes. *Trans. ASME, J.
Fluids Engrg.* 103: 162–69
Ahmed, S. R. 1984. Influence of base slant
on the wake structure and drag of road
vehicles. *Trans. ASME, J. Fluids Engrg.*
105: 429–34
Ahmed, S. R. 1992. Numerische Verfahren.
See Hucho 1992, Chap. 14
Ahmed, S. R., Hucho, W.-H. 1977. The cal-
culation of the flow field past a van with
the aid of a panel method. *SAE Pap. 770
390*
Ahmed, S. R., Ramm, R., Faltin, G. 1984.
Some salient features of the time averaged
ground vehicle wake. *SAE Pap. 840 300*
Aoki, K., Miyata, H., Kanai, M., Hanaoka,
Y., Zhu, M. 1992. A water-basin test tech-

nique for the aerodynamic design of road
vehicles. *SAE Pap. 920 348*
Barth, R. 1960. Der Einfluss unsym-
metrischer Stroemung auf die Luftkraefte
an Fahrzeugmodellen und aehnlichen
Koerpern. *Automobiltech. Z.* 62: 80–95
Basshuysen, R. v., Chemnitzer, E., Stock,
D. 1989. Der neue 3-m2- Klimawindkanal
mit Allrad-Rollenpruefstand bei Audi.
Automobiltech. Z. 91: 646–52
Bearman, P. W. 1984. Some observations on
road vehicle wakes. *SAE Pap. 840 301*
Beauvais, F. N., Tignor, S. C., Turner, T. R.
1968. Problems of ground simulation in
automotive aerodynamics. *SAE Pap. 680
121*
Buchheim, R., Deutenbach, K.-R., Lueck-
hoff, H.-J. 1981. Necessity and premises

for reducing the aerodynamic drag of future passenger cars. *SAE Pap. 810 185*

Buchheim, R., Dobrzynski, W., Mankau, H., Schwabe, D. 1983. Vehicle interior noise related to external aerodynamics. *Int. J. Veh. Des.* SP 3

Buchheim, R. Schwabe, D., Roehe, H. 1986. Der neue 6 m2- Klimawindkanal von Volkswagen. *Automobiltech. Z.* 88: 211–18, 389–92

Buchheim, R., Durst, F., Beeck, M. A., Hentschel, W., Piatek, R., Schwabe, D. 1987. Advanced experimental techniques and their application to automotive aerodynamics. *SAE Pap. 870 244*

Buchheim, R., Knorr, G., Mankau, H., Tang, T. 1989. Expertensystem zur Unterstuetzung der Aerodynamikoptimierung von Fahrzeugen. *GMD-Stud.* 160: 60–83

Carr, G. W. 1987. New MIRA drag reduction prediction method for cars. *Auto. Eng.* June/July 1987: 34–38

Cogotti, A. 1983. Aerodynamic characteristics of car wheels. *Int. J. Veh. Des.* SP 3: 173–96

Cogotti, A. 1987. Flow-field surveys behind three squareback car models using a new fourteen-hole probe. *SAE Pap. 870 243*

Cogotti, A. 1989. A strategy for optimum surveys of passenger-car flow fields. *SAE Pap. 890 374*

Cogotti, A., Berneburg, H. 1991. Engine compartment airflow investigations using a laser-doppler velocimeter. *SAE Pap. 910 308*

Dick, A., Stricker, R. 1988. Zur Bewertung inhomogenen Klimas im Pkw durch ein thermophysiologisches Insassenmodell. *VDI-Bere.* 699: 247–64, Duesseldorf

Donges, E., Mueller, B., Seifdenfuss, T. 1990. Design of the BMW-safety concept for active rear-axle kinematics. *23rd FISITA Congr., Torino,* Pap. 905 059

Eckert, W., Vagt, J.-D., Wolff, B. 1990. Die Messtrecke mit geschlitzten Waenden im Porsche Windkanal. *Automobiltech. Z.* 92: 286–97

Eckert, W., Singer, N., Vagt, J.-D. 1992. The Porsche wind tunnel floor-boundary-layer control—a comparison with road data and results from moving belt. *SAE Pap. 920 346*

Emmelmann, H.-J. 1987a. Driving stabilty in side winds. See Hucho 1987, Chap. 5

Emmelmann, H.-J. 1987b. Performance of cars and light vans. See Hucho 1987, Chap. 3

Emmelmann, H.-J., Berneburg, H., Schulze, J. 1990. Aerodynamic development of the Opel Calibra. *SAE Pap. 900 327*

Flegl. H., Rauser, M. 1992. Hochleistungsfahrzeuge. See Hucho 1992, Chap. 7

Gengenbach, W. 1987. Heating, ventilation and air conditioning of motor vehicles. See Hucho 1987, Chap. 10

George, A. R. 1989. Automobile aeroacoustics. *AIAA Pap.* 89–1067, San Antonio, TX

Gilhaus, A., Renn, V. 1986. Drag and driving-stability related aerodynamic forces and their interdependence—results of measurements on 3/8 scale basic car shapes. *SAE Pap. 860 211*

Gilhaus, A., Hoffmann, R. 1992. Richtungsstabilitaet. See Hucho 1992, Chap. 5

Glober, S., Rumez, W. 1990. Berechnung der Stroemung und Temperaturverteilung in Fahrzeugkabinen mit einem Navier-Stokes-Verfahren. *VDI-Ber.* 816: 335–44

Goehring, E., Kraemer, W. 1987. Seitliche Fahrgestellverkleidungen fuer Nutzfahrzeuge. *Automobiltech. Z.* 89: 481–88; 659–66

Goenka, L. N. 1990. A numerical model to determine vehicle pressure-simulation accuracy in a slotted-wall automotive wind tunnel. *SAE Pap. 900 188*

Hackett, J. E., Wilsden, D. J. 1975. Determination of low speed wake blockage correction via tunnel wall static pressure measurements. *AGARD Fluid Dynamics Panel, Symp. on Wind Tunnel Des. Testing Techniques, London*

Hackett, J. E., Sugavanam, A. 1984. Evaluation of a complete wake integral for the drag of a car-like shape. *SAE Pap. 840 577*

Haruna, S., Kamimoto, I., Okamoto, S. 1992. Estimation method for automobile aerodynamic noise. *SAE Pap. 920 205*

Hensel, R. W. 1951. Rectangular wind tunnel corrections using the velocity ratio method. *NACA TN 2372*

Hucho, W.-H. 1974. *Versuchstechnik in der Fahrzeugaerodynamik. Koll. Industrieaerodynamik, Teil 3: Aerodynamik von Strassenfahrzeugen.* Aachen

Hucho, W.-H. 1978. The aerodynamic drag of cars—current understanding, unresolved problems and future prospects. See Sovran et al 1978, pp. 7–44

Hucho, W.-H., ed. 1987a. *The Aerodynamics of Road Vehicles.* London: Butterworth

Hucho, W.-H. 1987b. Aerodynamic drag of passenger cars. See Hucho 1987a, Chap. 4

Hucho, W.-H. 1989a. Neuartiger Akustik-Windkanal bei BMW. *Auto. Rev.* 41/5.10.1989: 43–45

Hucho, W.-H. 1989b. Numerischer Windkanal—Stromlinienautos aus dem Supercomputer? *Comput. Technol.* 1989/10: 44–62

Hucho, W.-H., ed. 1992. *Aerodynamik des Automobils.* Duesseldorf: VDI. In press

Hucho, W.-H., Emmelmann, H.-J. 1973.

Theoretical prediction of the aerodynamic derivatives of a vehicle in cross wind gusts. *SAE Pap. 730 232*

Hucho, W.-H., Janssen, L. J., Schwarz, G. 1975. The wind tunnel's ground floor boundary layer—its interference with the flow underneath cars. *SAE Pap. 750 066*

Hucho, W.-H., Janssen, L. J., Emmelmann, H.-J. 1976. The optimization of body details—a method for reducing the aerodynamic drag of vehicles. *SAE Pap. 760 185*

Hucho, W.-H., Janssen, L. J. 1977. Flow Visualization techniques in vehicle aerodynamics. *Int. Symp. on Flow Visualization, Tokyo*

Hummel, D., Ramm, G. 1992. A panel method for the computation of the flow around vehicles including side-edge vortices and wakes. *Proc. ATA-Conf. Innovation and Reliability in Auto. Des. and Testing, Florence*

Hutchings, B. J., Pien, W. 1988. Computation of three-dimensional vehicle aerodynamics using FLUENT/BFC. See Marino 1988, pp. 233–55

Ishihara, Y., Hara, J., Sakamoto, H., Kamemoto, K., Okamoto, H. 1991. Determination of flow velocity distribution in a vehicle interior using visualization and computation techniques. *SAE Pap. 910 310*

Janssen, L. J., Hucho, W.-H. 1975. Aerodynamische Entwicklung von VW-Golf und VW-Scirocco. *Automobiltech. Z.* 77: 1–5

Jones, R. T. 1978. Discussion. See Sovran et al 1978, pp. 40–44

Kamm, W., Schmid, C., Riekert, P., Huber, L. 1934. Einfluss der Reichsautobahn auf die Gestaltung der Kraftfahrzeuge. *Automobiltech. Z.* 37: 341–54

Kataoka, T., China, H., Nakagawa, K., Yanagimoto, K., Yoshida, M. 1991. Numerical simulation of road vehicle aerodynamics and effect of aerodynamic devices. *SAE Pap. 910 597*

Kieselbach, R. J. F. 1982a. *Streamline Cars in Germany. Aerodynamics in the Construction of Passenger Vehicles 1900–1945.* Stuttgart: Kohlhammer Ed. Auto und Verk.

Kieselbach, R. J. F. 1982b. *Streamline Cars in Europe and USA. Aerodynamics in the Construction of Passenger Vehicles 1900–1945.* Stuttgart: Kohlhammer Ed. Auto und Verk.

Kieselbach, R. J. F. 1983. *Aerodynamically Designed Commercial Vehicles 1931–1961 Built on the Chassis of: Daimler Benz, Krupp, Opel, Ford.* Stuttgart: Kohlhammer Ed. Auto und Verk.

Klemperer, W. 1922. Luftwiderstandsuntersuchungen an Automodellen. *Z. Flugtech. Motorluftschiffahrt.* 13: 201–6

Kobayashi, T., Kitoh, K. 1992. A review of CFD methods and their application to automobile aerodynamics. *SAE Pap. 920 338*

Koenig-Fachsenfeld, R. v. 1951. *Aerodynamik des Kraftfahrzeugs.* Frankfurt: Umschau

Koenig-Fachsenfeld, R. v., Ruehle, D., Eckert, A., Zeuner, M. 1936. Windkanalmessungen an Omnibusmodellen. *Automobiltech. Z.* 39: 143–49

Krukow, G., Stricker, R. 1990. Einsatzpotential gekoppelter Verfahren zur Simulation von 3D-Fahrzeugstroemungen. *VDI Ber.* 816: 367–77, Duesseldorf

Kuenstner, R., Deutenbach, K.-R., Vagt, J.-D. 1992. Measurement of reference dynamic pressure in open-jet automotive wind tunnels. *SAE Pap. 920 344*

Kuriyama, T. 1988. Numerical simulation on three dimensional flow and heat transfer in the engine compartment using "STREAM." See Marino 1988, pp. 283–92

Larsson, L., Nilsson, L. U., Berndtsson, A., Hammar, L., Knutson, K., Danielson, H. 1989. A study of ground simulation-correlation between wind-tunnel and waterbasin tests of a full-scale car. *SAE Pap. 890 368*

Larsson, L., Broberg, L., Janson, C.-E. 1991. A zonal method for predicting external automoblie aerodynamics. *SAE Pap. 910 595*

Mackrodt, P.-A., Steinheuer, J., Stoffers, G. 1980. Entwicklung aerodynamisch optimaler Formen fuer das Rad/Schiene-Versuchsfahrzeug II. *Arch. Eisenbahntech.* 35: 67–77

Mackrodt, P.-A., Pfitzenmaier, E. 1987. Aerodynamik und Aeroakustik fuer Hochgeschwindigkeitszuege. *Phys. Unserer Zeit.* 18: 65–76

Marino, C., ed. 1988. Supercomputer applications in automotive research and development. *Proc. 2nd Int. Conf. on Supercomputing Appl. in the Auto. Ind., Seville.* Minneapolis: Cray Res.

Mercker, E. 1986. A blockage correction for automotive testing in a wind tunnel with closed test section. *J. Wind Eng. Ind. Aerodyn.* 22: 149–67

Mercker, E., Knape, H. W. 1989. Ground simulation with moving belt and tangential blowing for full scale automotive testing in a wind tunnel. *SAE Pap. 890 248*

Mercker, E., Wiedemann, J. 1990. Comparison of different ground simulation

techniques for use in automotive wind tunnels. *SAE Pap. 900 321*

Mercker, E., Breuer, N., Berneburg, H., Emmelmann, H.-J. 1991. On the aerodynamic interference due to the rolling wheels of passenger cars. *SAE Pap. 910 311*

Moerchen, W. 1968. The climatic wind tunnel of Volkswagenwerk AG. *SAE Pap. 680 120*

Morel, T. 1978a. The effect of base slant on the flow pattern and drag of three-dimensional bodies with blunt ends. See Sovran et al. 1978, pp. 191–226

Morel, T. 1978b. Aerodynamic drag of bluff body shapes characteristic of hatch-back cars. *SAE Pap. 780 267*

Nouzawa, T., Haruna, S., Hiasa, K., Nakamura, T., Sato, H. 1990. Analysis of wake pattern for reducing aerodynamic drag of notchback model. *SAE Pap. 900 318*

Nouzawa, T., Hiasa, K., Nakamura, T., Kawamoto, A. 1992. Unsteady-wake analysis of the aerodynamic drag of a notchback model with critical afterbody geometry. *SAE Pap. 920 202*

Ogata, N., Iida, N., Fuji, Y. 1987. Nissan's low-noise full scale wind tunnel. *SAE Pap. 870 250*

Ono, K., Himeno, R., Fujitani, K., Uematsu, Y. 1992. Simultaneous computation of the external flow around a car body and the internal flow through its engine compartment. *SAE Pap. 920 342*

Onorato, M., Costelli, A. F., Garrone, A. 1984. Drag measurement through wake analysis. *SAE Pap. 840 302*

Piatek, R. 1987. Operation, safety and comfort. See Hucho 1987a, Chap. 6

Piech, F. 1992. 3 Liter/100 km im Jahr 2000. *Automobiltech. Z.* 94: 20–23

Rauser, M., Eberius, J. 1987. Verbesserung der Fahrzeugaerodynamik durch Unterbodengestaltung. *Automobiltech. Z.* 89: 535–42

Retzlaff, R. N., Hertz, P. B. 1990. Airfoil plan-view body shapes to reduce drag at yaw. *SAE Pap. 900 314*

Rose, M. J. 1984. Appraisal and modification of an empirical method for predicting the aerodynamic drag of cars. *MIRA Released Rep.* 1984/1

SAE 1990. Aerodynamic testing of road vehicles: open-jet wind tunnel boundary interference. *SAE Inform. Rep. J* 2071

SAE 1991. Aerodynamic testing of road vehicles: closed-test-section wind tunnel boundary interference. *SAE Inform. Rep. J* 2085

Schaub, U. W., Olson, M. E., Raimondo, S. 1990. Correction of wind tunnel force data for yawed full and half-scale truck models using a modified pressure-signature method. *SAE Pap. 900 187*

Sorgatz, U., Buchheim, R. 1982. Untersuchungen zum Seitenwindverhalten zukuenftiger Fahrzeuge. *Automobiltech. Z.* 84: 11–18

Sovran, G. 1983. Tractive-energy-based formulae for the impact of aerodynamics on fuel economy over the EPA driving schedules. *SAE Pap. 830 304*

Sovran, G. 1984. The effect of ambient wind on a road vehicle's aerodynamic work requirement and fuel consumption. *SAE Pap. 840 298*

Sovran, G., Morel, T., Mason, W. T., eds. 1978. *Aerodynamic Drag Mechanisms of Bluff Bodies and Road Vehicles.* New York: Plenum

Sovran, G., Bohn, M. S. 1981. Formulae for the tractive-energy requirements of vehicles driving the EPA schedules. *SAE Pap. 810 184*

Squire, H. B., Pankhurst, R. C. 1952. *ARC CP* 80

Stafford, L. G. 1973. A numerical method for the calculation of the flow around a motor vehicle. *Proc. Adv. Road Veh. Aerodyn. BHRA Fluid Eng., Cranfield,* pp. 167–83

Stapleford, W. R., Carr, G. W. 1971. Aerodynamic noise in road vehicles. *MIRA Rep.* 1971/2

Stollery, J. L., Burns, W. K. 1969. Forces on bodies in the presence of the ground. *Proc. 1st Symp. on Road Veh. Aerodynam.,* London, Nov. 6–7

Tsuboi, K., Shirayama, S., Oana, M., Kuwahara, K. 1988. Computational study of the effect of base slant. See Marino 1988, pp. 257–72

Vagt, J.-D., Wolff, B. 1987. Das neue Messzentrum fuer Aerodynamik—Zwei neue Windkanaele bei Porsche. Teil 1: *Automobiltech. Z.* 89: 121–29; Teil 2: *Automobiltech. Z.* 89: 183–89

von Schulz-Hausmann, K., Vagt, J.-D. 1988. Influence of test section length and collector area on measurements in 3/4-open-jet automotive wind tunnels. *SAE Pap. 880 251*

White, R. G. S. 1967. A rating method for assessing vehicle aerodynamic drag coefficients. *MIRA Rep.* 167/9

Wiedemann, J. 1986. Optimierung der Kraftfahrzeugdurchstroemung zur Steigerung des aerodynamischen Abtriebes. *Automobiltech. Z.* 88: 429–31

Wiedemann, J., Ewald, B. 1989. Turbulence

manipulation to increase effective Reynolds numbers in vehicle aerodynamics. *AIAA J.* 27: 763-69

Williams. J. E., Hackett, J. E. Oler, J. W. Hamar, L. 1991. Water flow simulation of automotive underhood airflow phenomena. *SAE Pap. 910 307*

Willumeit, H. P., Matheis, A., Mueller, K. 1991. Korrelation von Untersuchungsergebnissen zur Seitenwindempfindlichkeit eines Pkw im Fahrsimulator und Prueffeld. *Automobiltech. Z.* 93: 28–35

Wright, P. G. 1983. The influence of aerodynamics on the design of Formula-One racing cars. *Int. J. Veh. Des.*, SP 3: 158–72